

POLITECNICO DI TORINO

Master of Science in Mechanical Engineering

MASTER'S THESIS



Development and testing of an automatic modal parameters identification method

Supervisor:
Prof. Alessandro Fasana

Candidate:
Donato Foggetti

Academic Year 2017-2018

Contents

Abstract	v
Introduction	1
1 State of art	3
2 EMA method development	5
2.1 Software overview	5
2.2 Computation	5
2.2.1 Mode detection and extraction of the singular values . . .	9
2.2.2 Conversion from frequency to time domain	9
2.2.3 Computation of the modal damping ratio	10
2.3 PSD fitting	15
2.4 MIMO systems	17
2.4.1 Vector tracking	17
2.5 Symmetric structures	19
2.6 C++ implementation	21
2.7 Automation of the procedure	22
2.7.1 In-depth analysis	22
2.7.2 Mode shapes plots	26
2.8 Testing	27
2.8.1 Lumped parameters numerical system	28
2.8.2 Continuous numerical system	32
2.8.3 Steel plate	42
3 EMA and OMA comparison	47
3.1 Basic concepts	47
3.2 Description of the comparison	48
3.3 Results	48
Bibliography	52

List of Figures

1	Basic representation of identification methods classification. . . .	2
1.1	An example of the cross singular value or eigenvalue effect and the result after vector tracking on a 15 DOF structure [2].	4
2.1	The GUI as it appears when opened.	7
2.2	The GUI with 7 SISO FRFs loaded.	7
2.3	The GUI with 7 SISO FRFs and the resulting SIMO one.	8
2.4	The GUI with the CMIF plot.	8
2.5	The GUI at the end of the analysis.	9
2.6	Graphical output for an investigated mode.	12
2.7	An example to show that time domain signals reconstructed from real data don't have a constant decay rate.	14
2.8	PSD fitting graphical output: in black the original curve and in red the fitted one. In this case (mode 1) they are almost superimposed.	16
2.9	A simplified scheme of the 3D matrix.	17
2.10	The GUI with the CMIF plot of a MIMO system.	18
2.11	A simplified scheme of the matrix containing the singular vectors.	19
2.12	On the dotted plot MATLAB <i>datatips</i> can be used in order to read the index of the chosen point.	21
2.13	CMIF plot with Modal Coherence: threshold, intervals limits and peaks are highlighted.	25
2.14	MAC matrix of the aluminium plate with 12 input and 7 output channels.	26
2.15	15 DOFs numerical system scheme [2].	29
2.16	CMIF plot with Modal Coherence of the 15 DOFs system with 15 input and output channels.	30
2.17	MAC matrix of the 15 DOFs system with 15 input and output channels.	31
2.18	MAC matrix before and after the last check.	31

2.19	CMIF plot with Modal Coherence of the 15 DOFs system with 15 input channels and 2 output channels: only 4 out of 15 modes have been detected.	32
2.20	FE model with node numbers.	33
2.21	CMIF plot with Modal Coherence of the FE model (low damping): 6 out of 8 modes have been automatically detected.	36
2.22	MAC matrix before and after the last check.	36
2.23	CMIF plot with Modal Coherence of the FE model (medium damping): 6 out of 8 modes have been automatically detected.	37
2.24	MAC matrix before and after the last check.	38
2.25	CMIF plot with Modal Coherence of the FE model (high damping): 5 out of 8 modes have been automatically detected.	39
2.26	MAC matrix	39
2.27	Modes 1 to 4.	40
2.28	Modes 5 to 8.	41
2.29	Test setup with 40 impact points and 7 output channels.	43
2.30	MAC matrix of the steel plate with 40 impact points and 7 output channels.	44
2.31	CMIF plot with Modal Coherence of the steel plate with 40 impact points and 7 output channels.	44
2.32	Test setup with 35 impact points and 2 output channels.	45
2.33	MAC matrix before and after the last check.	45
2.34	CMIF plot with Modal Coherence of the steel plate with 35 impact points and 2 output channels.	46
3.1	DOFs information assigned in <i>ARTEMIS Modal</i>	48
3.2	<i>ARTEMIS Modal</i> screenshots showing the geometry and the channels in the OMA measurements.	49

List of Tables

2.1	Summary of the results obtained by using the logarithmic decrement method (SIMO).	13
2.2	Summary of the results obtained by using the linear fitting method (SIMO).	13
2.3	Summary of the results obtained by using the PSD fitting method (SIMO).	16
2.4	Summary of the results obtained by using the logarithmic decrement method (MIMO).	19
2.5	Summary of the results obtained by using the linear fitting method (MIMO).	20
2.6	Summary of the results obtained by using the PSD fitting method (MIMO).	20
2.7	15 DOFs system results with 15 input and output channels.	30
2.8	FE model (low damping) results.	35
2.9	FE model (medium damping) results.	37
2.10	FE model (high damping) results.	38
2.11	Steel plate results with 40 impact points and 7 output channels.	43
2.12	Steel plate results with 35 impact points and 2 output channels.	46
3.1	Comparison between RFP-Z and EFDD.	50
3.2	Comparison between RFP-Z and SSI-UPCX.	50

Abstract

In the last century, researchers and scholars focused on studying dynamic effects on buildings and machines. This big effort led to a wide variety of analysis methods, that can be collected in two big categories: Operational and Experimental Modal Analysis. Nowadays a lot of commercial softwares are equipped with several different methods in order to give the best results in every situation and the trend tends to the development of routines that are always more automatic in order to be simple and quick to use.

In this work a fully automatic EMA method will be developed and tested with both numerical and real systems. In the last Chapter, a comparison between EMA and OMA on a real structure has been carried out and commented.

Nomenclature

ω = general frequency variable (*rad/s*).

ω_r = natural frequency related to the mode r (*rad/s*).

ω_d = damped frequency (*rad/s*).

ζ_r = damping ratio related to the mode r .

$\{\psi_r\}$ = eigenvector related to the mode r (mode shape vector).

$\{\phi_r\}$ = modal mass scaled eigenvector related to the mode r .

$[\Psi]$ = modal matrix.

$[M]$ = mass matrix.

$[C]_p$ = proportional damping matrix.

$[K]$ = stiffness matrix.

$[\bar{M}]$ = modal mass matrix (diagonal).

$[\bar{C}]$ = modal damping matrix (diagonal).

$[\bar{K}]$ = modal stiffness matrix (diagonal).

f_s = sampling frequency (*Hz*).

$[H]$ = FRF matrix.

λ = eigenvalue.

$[\Sigma]$ = singular values matrix (diagonal).

$[U]$ = left singular vector matrix.

$[V]$ = right singular vector matrix.

$[]^T$ = transpose of a matrix.

$[]^H$ = hermitian of a matrix (transpose and complex conjugated).

N_i = number of input channels.

N_o = number of output channels.

N_{SV} = number of singular values.

K = number of samples in the analysed spectrum.

Introduction

In the last decades an always greater interest in structural dynamics has grown, both in Mechanical and Civil Engineering. This happened for several reasons, like avoiding failures due to fatigue and resonances of structures and rotors or improving comfort in vehicle cabins (NVH) and so on.

For this reason, through the years, a large number of researchers have worked to develop different methods in order to fit the majority of cases and situations.

The most used approach to dynamic analysis of structures is *modal analysis* and its aim is the conversion of a MDOF (**M**ultiple **D**egrees **O**f **F**reedom) system with n DOFs in n SDOF (**S**ingle **D**egree **O**f **F**reedom) ones. In this way the estimation, or *identification*, of the modal parameters, that are natural frequencies ω_r , damping ratios ζ_r and mode shapes $\{\psi_r\}$, becomes possible.

In this context, two main categories of modal analysis were born: the OMA (**O**perational **M**odal **A**nalysis) and the EMA (**E**xperimental **M**odal **A**nalysis).

The main difference between the two kinds of analysis is the nature of the used data: in EMA the classic FRFs (**F**requency **R**esponse **F**unctions) are used, that carry information about both the input excitation and the measured output response, while in OMA only the output response is measured and processed.

This OMA peculiarity makes it especially suitable for the analysis of structures in their real working conditions, advantage that is very important for big or heavy structures that can not be brought in a laboratory or in all the situations in which the input is impossible to measure. In these conditions, the input has to satisfy some requirements, but basically it has to be a white noise [1]. Besides this, since the aim is to study structures in their real operating conditions, it is not necessary to isolate them from external excitations, so a test rig is not required.

On the other hand, in EMA, a test rig is always required and this often carries improper boundary conditions issues, that, with improper excitation levels have to be accepted. Last but not least, also shakers and hammers limits have to be taken into account.

Actually, this is not the only classification for identification methods. They can also be subdivided between time domain methods and frequency domain ones, methods for MDOF systems and methods for SDOF ones. The complete classification is reported in Figure 1.

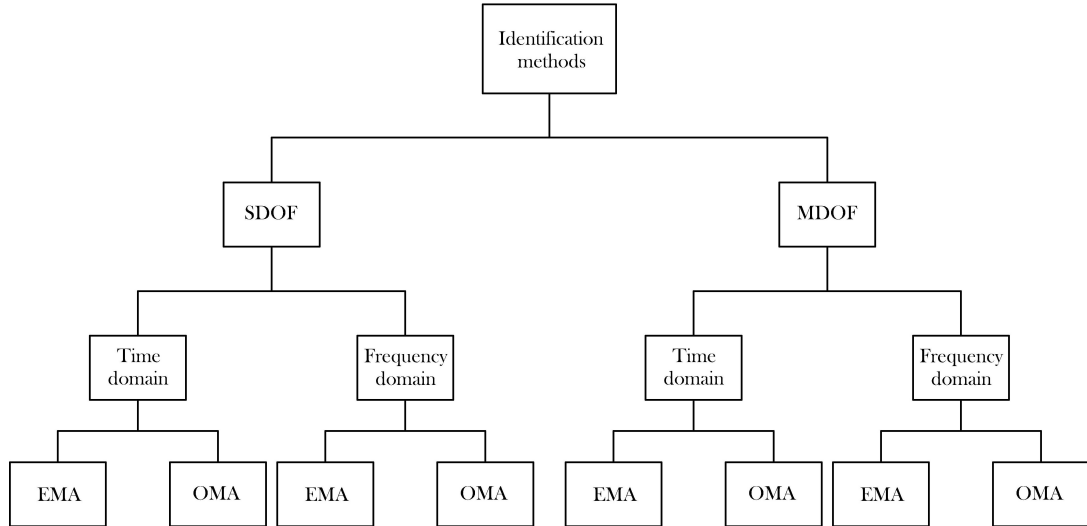


Figure 1: Basic representation of identification methods classification.

In Chapter 1 the context in which this work is carried on is explained; in Chapter 2 the development of a fully automatic EMA method will be described and some test results are shown; in Chapter 3 a comparison between EMA and OMA on a practical case will be carried out and commented.

Chapter 1

State of art

Today a lot of methods for EMA are available, for example the logarithmic decrement method (SDOF, time domain), the Half-Power, or " -3 dB ", one (mainly SDOF, frequency domain), the more sophisticated Kennedy and Pancu method (SDOF extendible to MDOF, frequency domain) and so on.

The methods above are quite simple to use and usually don't require a deep manipulation of the signal, in fact they just use different graphic representations of the response to extract the modal parameters. As an example, the Half-Power method uses the classic representation of the FRF in the amplitude-frequency plane with the first expressend in dB , whereas the Kennedy and Pancu one needs the FRF to be plotted as a Nyquist plot.

The most modern techniques use different mathematical tools. One of the most commonly used among them in the last twenty years is the so called CMIF (**C**omplex **M**ode **I**ndicator **F**unction) [2]. It is based on the SVD (**S**ingular **V**alues **D**ecomposition) of the FRF matrix, defined as:

$$[H(\omega)] = [U(\omega)] [\Sigma(\omega)] [V(\omega)]^H \quad (1.1)$$

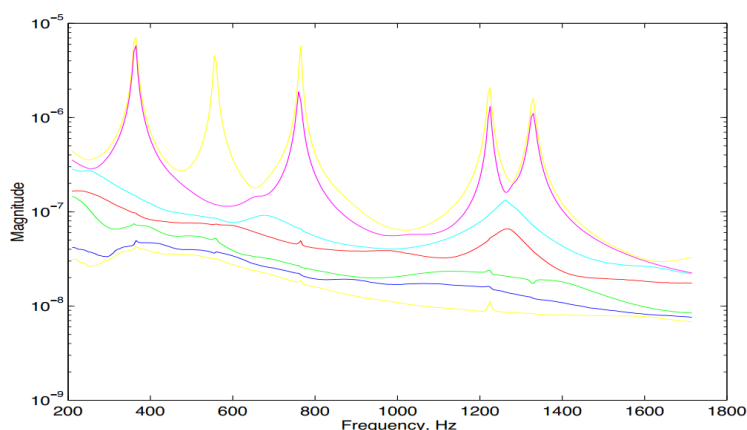
where $[H]$ is the FRF matrix, $[\Sigma]$ is the diagonal singular values matrix ($\Sigma_k^2 = \lambda_k$), $[U]$ is the left singular vector matrix and $[V]$ is the right singular vector matrix. The SVD of the FRF matrix is evaluated at each spectral line and by plotting the resulting singular values on a linear or logarithmic magnitude scale as a function of the frequency a CMIF plot is obtained. This curve is proportional to the classic FRF and brings the same information in terms of frequencies and magnitude: a peak in the plot indicates the location on the frequency axis that is the nearest to the frequency of the pole, with an error equal to the frequency resolution. The detected frequency is the damped frequency ω_d of the corresponding mode, defined

as it follows:

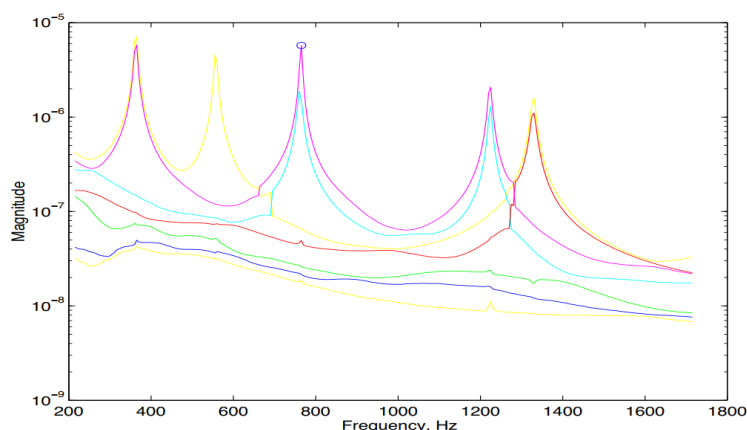
$$\omega_{d,r} = \omega_r \sqrt{1 - \zeta_r^2}. \quad (1.2)$$

The above explained method has some problems when more CMIFs are plotted. The algorithm, in fact, plots the singular values in decreasing order and in this way each obtained curve never crosses the others. This problem, known as *cross singular value or eigenvalue effect*, can be solved by using the *vector tracking*. The easiest implementation consists in evaluating the MAC (Modal Assurance Criterion) matrix between the singular vectors $\{U\}$ related to two consecutive spectral lines from zero to the Nyquist frequency. In this way, by watching the maximum value of the MAC matrix, it is possible to reconstruct the real CMIF plot, as shown in Figure 1.1.

Starting from the CMIF plot it is possible to fit a SDOF FRF to each peak, obtaining the so called eFRFs (enhanced FRFs), but this goes beyond the aims of this work.



(a) CMIF plot before vector tracking.



(b) The same plot after vector tracking.

Figure 1.1: An example of the cross singular value or eigenvalue effect and the result after vector tracking on a 15 DOF structure [2].

Chapter 2

EMA method development

2.1 Software overview

A CMIF based peak-picking identification method, applicable to SDOF and MDOF systems with any number of inputs and outputs, has been developed in order to be included in the commercial software *ARTEMIS Modal*, produced and distributed by *Structural Vibration Solutions A/S* (Aalborg, DK).

This software contains several EMA and OMA methods and specifically for the first category two of them are present: RFP-Z (**R**ational **F**raction **P**olynomial-**Z** domain), that is based on the stabilisation diagram and extracts natural frequencies, modal damping ratios and mode shapes, and the CMIF one, that extracts damped frequencies and mode shapes only. For this reason, finding a solution to compute the damping ratios has been the first goal of this work, in order to give to the user two alternative ways to identify the modal parameters. *ARTEMIS Modal*, in fact, with its *Validation module*, gives the opportunity to compare results coming from different methods, so that the user can critically choose the best ones and know how much reliable they are.

2.2 Computation

The idea behind the developed method is the isolation of the different modes in order to treat them as several SDOF systems.

A MATLAB program has been created. This program is equipped with a GUI (**G**raphic **U**ser **I**nterface), shown in Figure 2.1, that in first instance allows the user to load FRF data stored in files with different extensions, like Universal File Format (*.uff and *.unv) and the MATLAB one (*.mat).

Once the data are loaded, the software automatically recognises the number of input and output channels (respectively N_i and N_o) and can carry out different operations, like merging them to obtain SIMO (**S**ingle **I**nput **M**ultiple **O**utput) or MIMO (**M**ultiple **I**nput **M**ultiple **O**utput) data from SISO (**S**ingle **I**nput **S**ingle **O**utput) ones. It is important to remark that in order to extract the left singular vectors $\{U\}$ it is necessary to have at least one input and two outputs, obtaining singular vectors with dimension 2-by-1.

When more SISO dataset in MATLAB file format are loaded is it possible to obtain a SIMO dataset by selecting them and clicking on “Merge outputs”: in this way all the data are stored in a matrix in which each row contains the complex data coming from one accelerometer, so that the number of rows is equal to the number of outputs and the number of column is equal to the number of samples that are present in the analysed spectrum K . Obviously it is strictly necessary that data come from measurements carried out with the same sampling frequency and for the same time period in order to be merged.

After loading the data (Figure 2.2) and after building a SIMO dataset (Figure 2.3), it is possible to perform the SVD of the FRF for each spectral line simply by clicking on “SVD-FRF”, obtaining a CMIF interactive plot (Figure 2.4) with a frequency axis that goes from zero to the Nyquist frequency.

On this plot the user can select the peak that he wants to investigate on the curve by clicking with the left mouse button. A green circle on the peak indicates that it has been successfully selected.

In order to run the analysis it is sufficient to click with the right mouse button on the green circle and a red ring around it indicates that the analysis has been successfully carried out.

From the computational point of view, the calculation can be divided in some steps:

- 1) detection of the points of the curve that are affected mainly by the selected mode;
- 2) extraction of the corresponding singular values;
- 3) conversion of the frequency domain signal into a time domain one;
- 4) computation of the modal damping ratio using the logarithmic decrement method.

In the following pages, some screenshots of the GUI are reported. The processed data come from a numerical example, consisting in a 7 DOFs system.

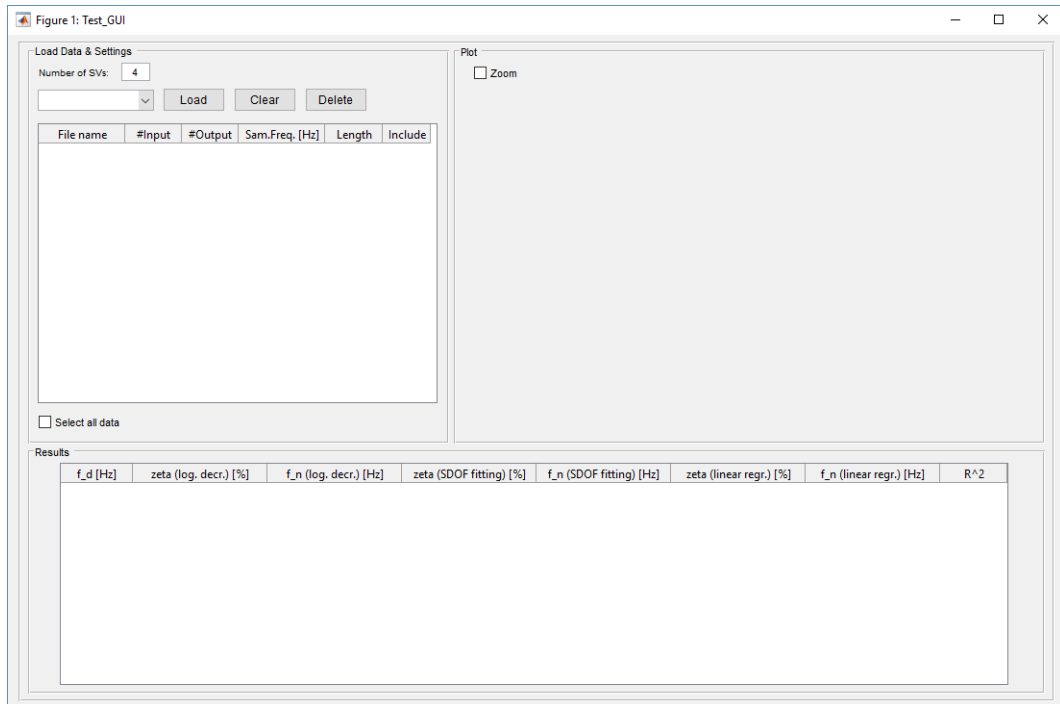


Figure 2.1: The GUI as it appears when opened.

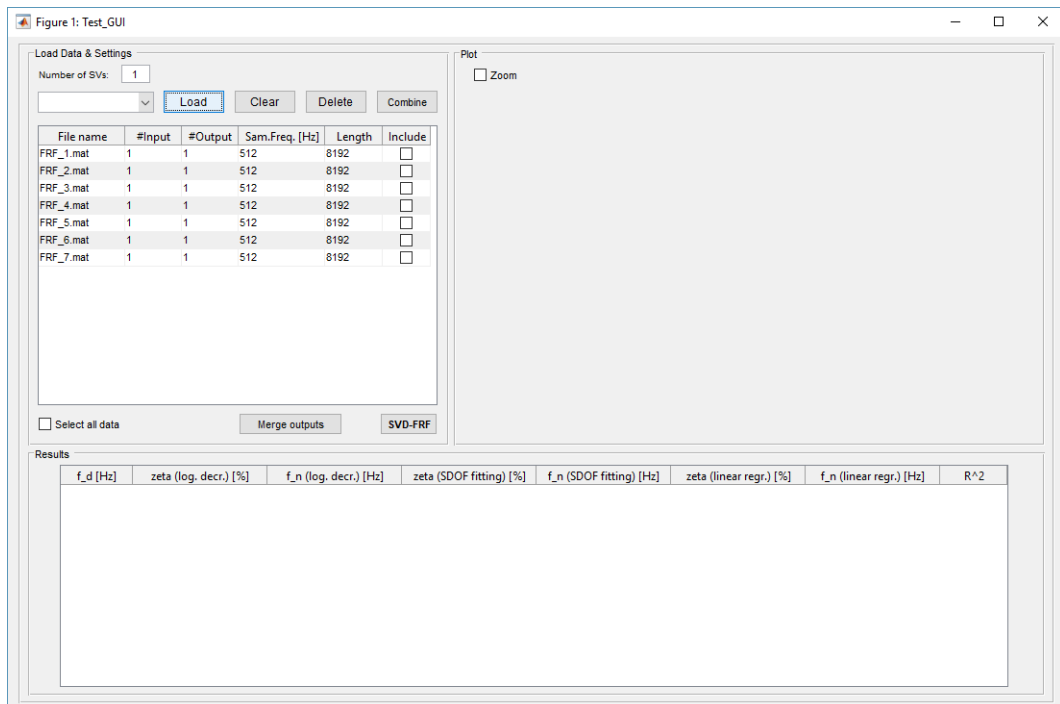


Figure 2.2: The GUI with 7 SISO FRFs loaded.

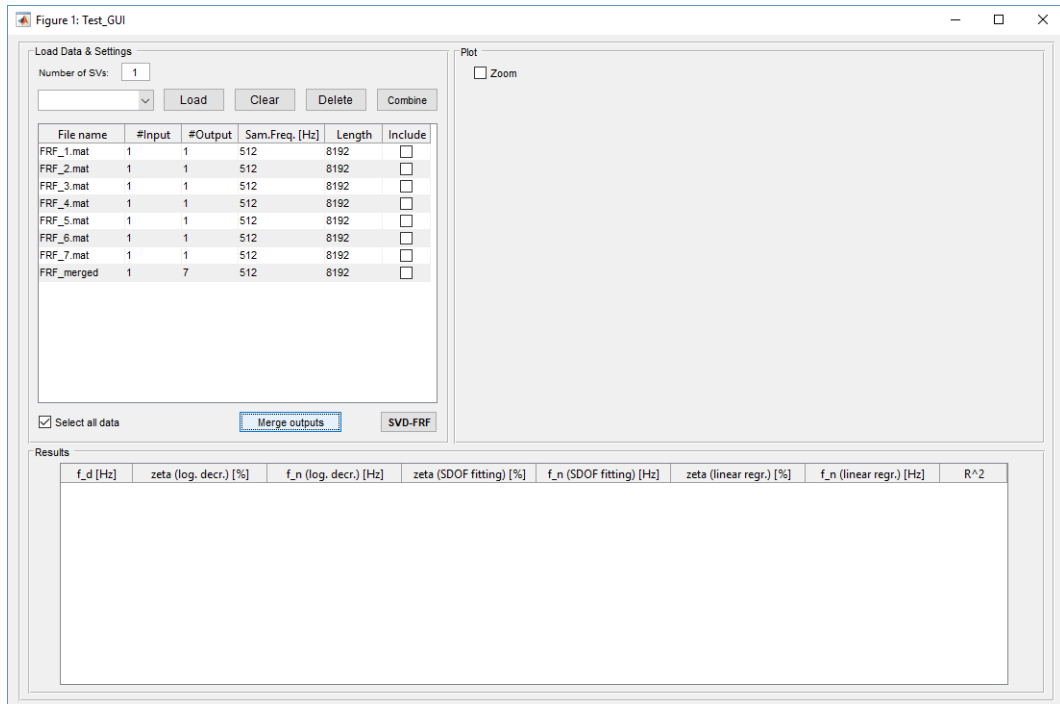


Figure 2.3: The GUI with 7 SISO FRFs and the resulting SIMO one.

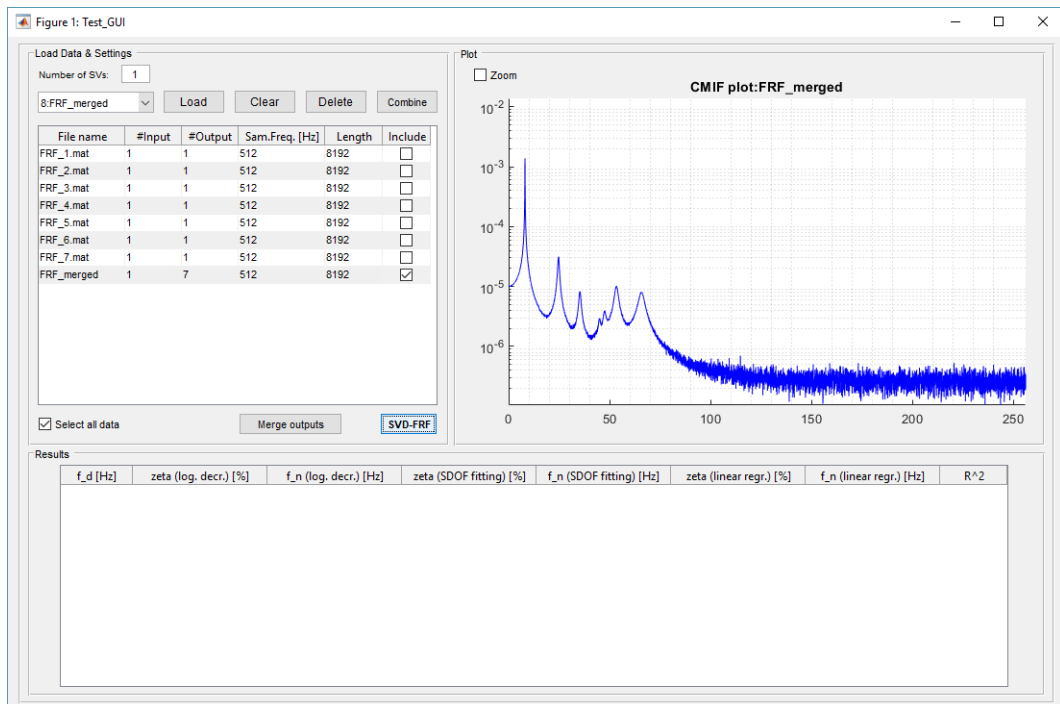


Figure 2.4: The GUI with the CMIF plot.

2.2.1 Mode detection and extraction of the singular values

Once a peak has been selected and the analysis is started, the software saves the corresponding singular value, singular vector and frequency.

Then, from this singular value the algorithm starts moving forward and backward on the frequency axis comparing, at each iteration, the singular vector corresponding to the selected spectral line with the one of the investigated singular value. This comparison is based on the calculation of the MAC, defined as follows [3]:

$$MAC(\{U_r\}, \{U_s\}) = \frac{|\{U_r\}^H \{U_s\}|^2}{(\{U_r\}^H \{U_r\})(\{U_s\}^H \{U_s\})} \quad (2.1)$$

The user can set the minimum admissible MAC and at this point the software detects the part of the curve that is affected mainly by the mode corresponding to the selected peak. A graphical output is also provided: all the accepted singular values are marked with a red dot as shown in Figure 2.5. All the results that will be shown have been calculated with a minimum admissible MAC equal to 0.8.

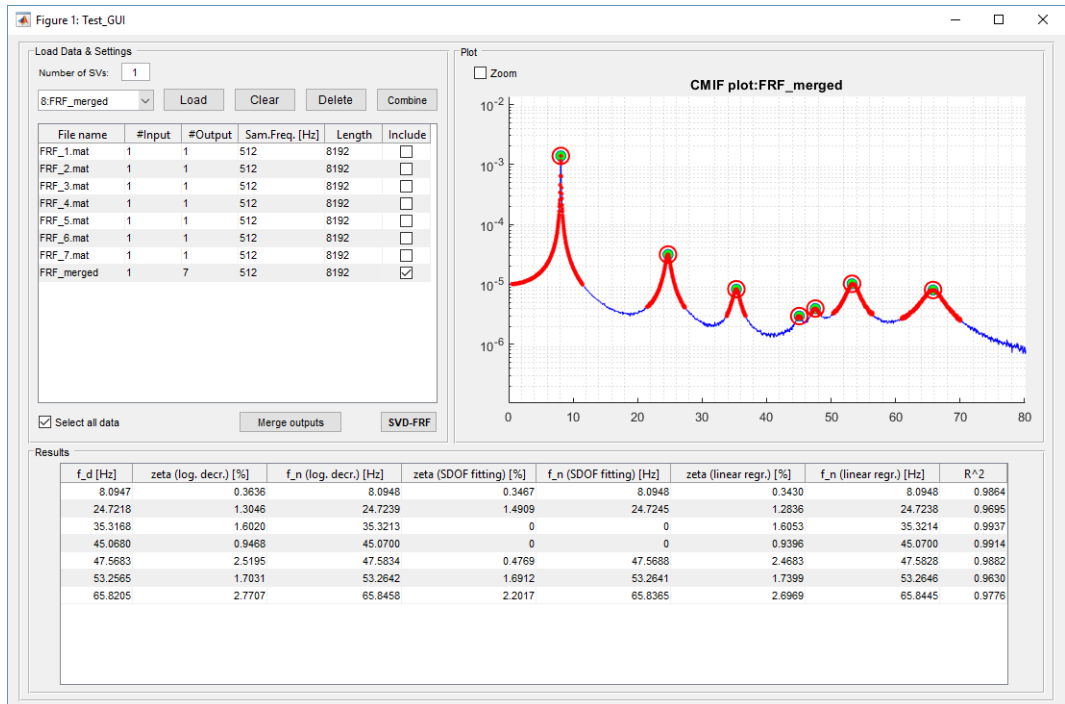


Figure 2.5: The GUI at the end of the analysis.

2.2.2 Conversion from frequency to time domain

At this point, the extracted singular values are saved in a vector of the same length of the FRF, which was initially full of zeros.

In order to obtain the time domain signal, this vector needs some manipulations: calling n its length, a null vector with length $2(n - 1)$ is created and the singular values are inserted in its first n positions. The remaining $n - 2$ elements should be complex and conjugated with respect to those from 2 to $n - 1$, that means that their real parts should be symmetric with respect to the element in the middle and the imaginary parts should be symmetric as well but opposite in sign.

The time domain signal is obtained by using the `ifft` MATLAB command, that performs the Inverse Fast Fourier Transform. This function requires in input a complex valued vector, while the singular values are real valued. For this reason, as a first attempt, a phase of zero has been introduced in each point, that is equivalent to setting a null imaginary part to the singular values.

The obtained time domain signal doesn't result very clear due to some beatings introduced by the quick jumps of the reconstructed SDOF FRF on both sides of the selected peak. In order to avoid this problem, before the IFFT, the peak extracted from the CMIF plot has been linked to the other elements of the vector, that are equal to zero, with a smooth curve. Such a link is constructed by computing the ratio between the first two points on the left and the last two points on the right that are different from zero and then on both sides other values are added maintaining the same ratio between two consecutive points. This is not strictly correct, due to the fact that the curve should have a horizontal asymptote at low frequencies corresponding to the static compliance (in case the FRF is a receptance) or an unpredictable behaviour at high frequencies (in case the FRF is an inertance). Such a kind of information is unknown, so the curves at both sides of the peak tend to zero.

2.2.3 Computation of the modal damping ratio

With these modifications, the beating in the time domain signal results less important and a first approximation of the modal damping ratio ζ_r can be computed by using the logarithmic decrement method [1].

As already stated, this is a very simple time domain method: it is sufficient to read on the plot the amplitude of two maxima n periods away one from the other. Calling x_1 the amplitude of the first maximum and x_n the one related to the maximum n periods away on the right, the logarithmic decrement δ is defined as it follows:

$$\delta = \ln \frac{x_1}{x_n} \quad (2.2)$$

and the modal damping ratio ζ_r is computable by using the following equation:

$$\zeta_r = \frac{\delta}{\sqrt{4n^2\pi^2 + \delta^2}} \quad (2.3)$$

Since the reconstructed time domain signal is computed from real frequency data, it is symmetrical with respect to the middle point, so the first half of the curve decreases with a higher rate with respect to the real one. For this reason the damping ratio is divided by 2, obtaining the final value.

With ζ_r it is possible to compute the natural frequency of the mode ω_r by inverting Equation (1.2).

Once a peak has been selected and analysed, a graphical output is available: the user can see the frequency domain signal before and after the correction of both the tails, the time domain one and the logarithm of the absolute value of its first half. Then, in order to apply the logarithmic decrement method, two thresholds are set, the highest one at the 80% of the first local maximum, the lowest one at its 10%. These thresholds are used to automatically choose the first and the last maximum to be used for the computation. Both the thresholds and the chosen maxima are shown in the provided graphical output, as shown in Figure 2.6.

In Figure 2.5 the GUI at the end of the analysis is shown: all the peaks have been picked and the results are listed in the table.

In Table 2.1 the obtained results are compared to the reference parameters of the analysed system, that are known. As regards the natural frequencies, the calculated values can be considered fully acceptable, while some damping ratios show a non-negligible difference from the reference value.

The damping ratio related to the first mode, for example, shows a difference from the reference value of 65.3%, that is not so large in an absolute scale, considering the fact that the value of the damping itself is very small. It can be stated that it probably occurs because the first mode is characterised by a very small damping. For what concerns the fifth mode, one probable reason of error is the fact that it is not characterised by a big amount of energy, so that the peak is not very high. Finally, for what concerns the seventh mode, it has been noticed that the error occurs due to the correction of the frequency domain signal, that causes some irregularities on both the sides; it is sufficient to change the value of the minimum admissible MAC in order to obtain a better result.

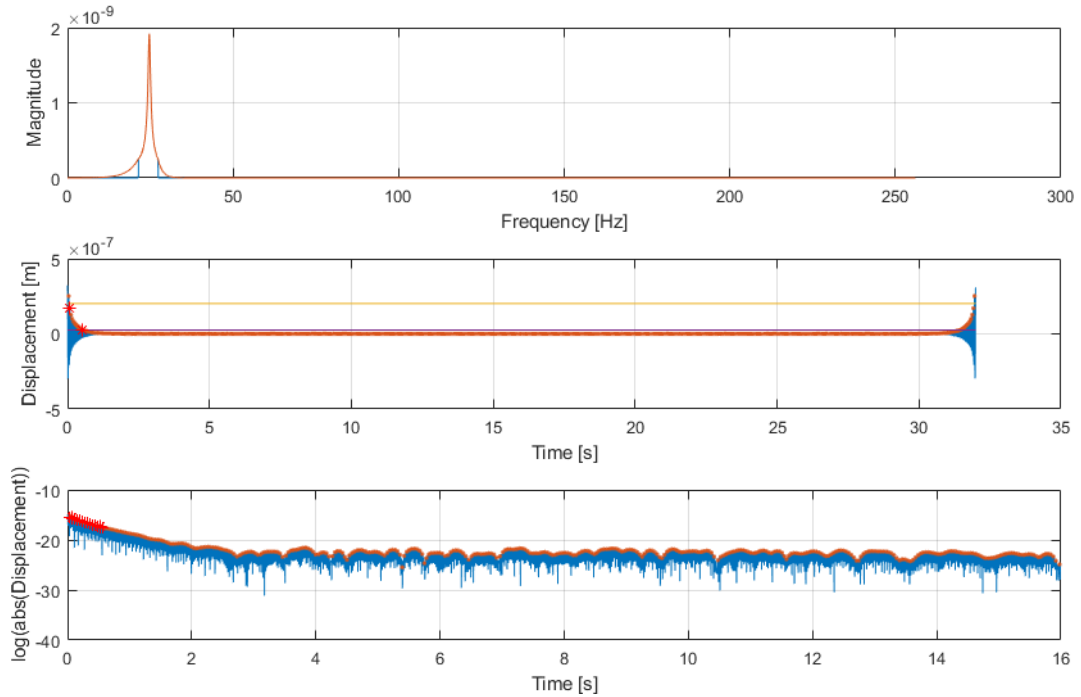


Figure 2.6: The graphical output: on the first plot the original frequency domain signal (blue) and the corrected one (orange) are visible; in the remaining plots, the time domain signal is reported in the two explained ways, with the chosen maxima, the thresholds and the fitted straight line highlighted.

Since the time domain signal (Figure 2.6) is obtained from real frequency data, it does not represent the exact time history: it is evident that the signal decreases and increases again and this is not correct. Besides this, the decreasing part has not a constant decay rate, so the computed damping ratio is strongly influenced by the choice of the first maximum and the number of periods n , influenced by the imposed thresholds.

This effect can be easily noticed by plotting the logarithm of the absolute value of the first half of the time domain signal and this is the reason why this kind of plot is provided in the graphical output: the decay should be exponential, so in this plot the maxima should be linked by a straight line. Figure 2.7 shows that this does not happen when real data are used to obtain the time domain signal by analysing a numerical SDOF system as example. On the vertical axis of the third plot it can be also noticed how the amplitude has been altered during the execution of `ifft` and this can be considered as another warning of the wrong reconstruction of the signal.

A possible way to simplify the problem is the approximation of the curve that links the maxima that are taken into account for the calculation with a straight

Mode	Natural frequency [Hz]		Damping ratio [%]		
	Reference	Experimental	Reference	Experimental	Δ [%]
1	8.09	8.09	0.22	0.36	65.3
2	24.70	24.72	1.44	1.30	9.4
3	35.32	35.32	1.43	1.60	12.0
4	45.03	45.07	1.15	0.95	17.7
5	47.55	47.58	1.38	2.52	82.6
6	53.46	53.26	1.61	1.70	5.8
7	65.99	65.85	1.97	2.77	40.6

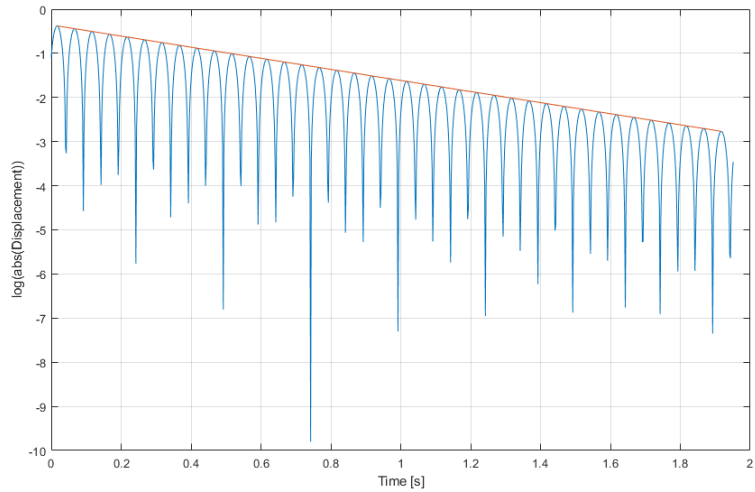
Table 2.1: Summary of the results obtained by using the logarithmic decrement method (SIMO).

line using MATLAB *Curve Fitting Tool* and the calculation of the damping ratio ζ as the mean value of all the damping ratios obtained with different numbers of periods n . The fitting has been performed by means of the function `fit`, that gives as output the coefficients of the straight line in the form $y = mx + q$, R^2 and other parameters out of the aim of this work. In the third plot of Figure 2.6 the fitted straight line can be slightly seen. In the GUI the result given from this method is reported as well, with also the value of R^2 as a parameter to evaluate the goodness of the linear regression.

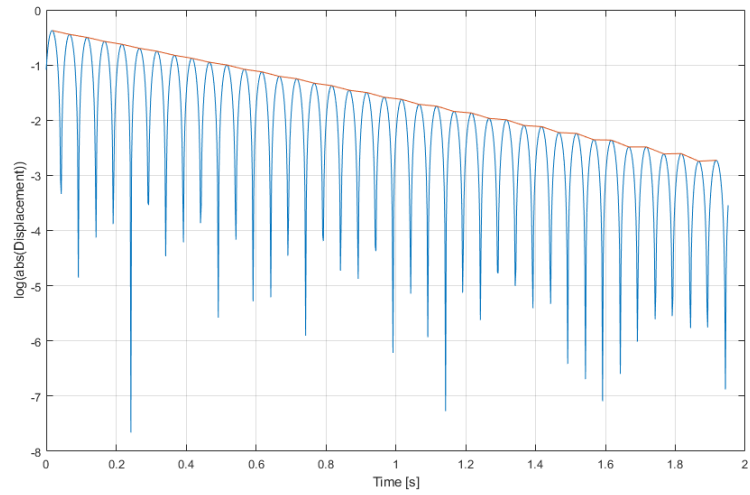
Table 2.2 shows the results of this method.

Mode	Natural frequency [Hz]		Damping ratio [%]			R^2
	Reference	Experimental	Reference	Experimental	Δ [%]	
1	8.09	8.09	0.22	0.34	55.9	0.986
2	24.70	24.72	1.44	1.28	10.9	0.970
3	35.32	35.32	1.43	1.61	12.3	0.994
4	45.03	45.07	1.15	0.94	18.3	0.991
5	47.55	47.58	1.38	2.47	78.9	0.988
6	53.46	53.26	1.61	1.74	8.1	0.963
7	65.99	65.84	1.97	2.70	36.9	0.978

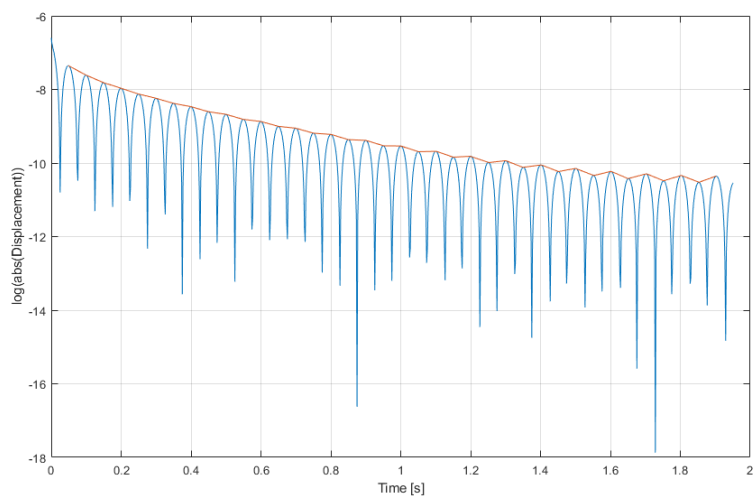
Table 2.2: Summary of the results obtained by using the linear fitting method (SIMO).



(a) Original time domain signal.



(b) Time domain signal reconstructed from complex data: some numerical errors can be seen at lower amplitudes.



(c) Time domain signal reconstructed from real data: the orange line is no more straight.

Figure 2.7: An example to show that time domain signals reconstructed from real data don't have a constant decay rate.

2.3 PSD fitting

Another method can be used in order to identify the modal parameters. Once the singular values are extracted according to the MAC value between their left singular vectors, they can be manipulated as if they were the actual FRF of the system.

The chosen points are used to fit a SDOF system FRF in order to use it to compute the damping ratio and the natural frequency with a method that relies on at least four spectral lines [4]. This method requires the expression of $H(\omega)$, that is the Fourier transform of the impulse response function $h(t)$, in the Z-domain and afterwards a least square solution is found in order to fit a SDOF system FRF to the selected points. Some details about the method will be now given.

In the Z-domain, the Fourier transform of the discrete impulse response function of a MDOF model is:

$$H_k = \sum_{r=1}^{2n} A_r \frac{z_k}{z_k - z_r} \quad (2.4)$$

where z_r is related to the system poles $s_r = -\zeta_r \omega_r \pm i \omega_r \sqrt{1 - \zeta_r^2}$. If the modes are well separated, a SDOF model can be assumed. This is equivalent to assume $n = 1$ in Equation (2.4), that becomes:

$$H_k = \frac{b_1 z_k + b_2 z_k^2}{a_0 + a_1 z_k + z_k^2} \quad (2.5)$$

where a_0, a_1, b_1 and b_2 are real. After some algebraic passages, it is possible to express:

$$|H_k|^2 = \frac{1 + A \cos x_k}{B + C \cos x_k + D \cos 2x_k} \quad (2.6)$$

with A, B, C and D real coefficients. With the assumption of input with flat spectrum in the frequency range of interest, it is possible to state that $S_{yy} \propto |H_k|^2$ and then it is possible to write Equation (2.6) for each spectral line k . Since the unknowns are just four, it is possible to find a least square solution for A, B, C and D and from them a_0 and a_1 can be computed. As last step, ω_r and ζ_r can be found:

$$\omega_r = \sqrt{\left[f_s \arccos \left(-\frac{1}{2} \frac{a_1}{\sqrt{a_0}} \right) \right]^2 + \left(\frac{f_s}{2} \ln(a_0) \right)^2} \quad (2.7)$$

$$\zeta_r = \left(-\frac{f_s}{2} \ln(a_0) \right) / \omega_r \quad (2.8)$$

Mode	Natural frequency [Hz]		Damping ratio [%]		
	Reference	Experimental	Reference	Experimental	Δ [%]
1	8.09	8.09	0.22	0.35	57.6
2	24.70	24.72	1.44	1.49	3.5
3	35.32	-	1.43	-	-
4	45.03	-	1.15	-	-
5	47.55	47.58	1.38	0.48	65.4
6	53.46	53.26	1.61	1.69	5.0
7	65.99	65.85	1.97	2.20	11.8

Table 2.3: Summary of the results obtained by using the PSD fitting method (SIMO).

In Table 2.3 some results from the same data of the previous Paragraph are shown.

From modes 2 and 6 it can be noticed that this method gives better results, since it does not involve the conversion into a time domain signal, that is the part that introduces errors in the previously described method. Anyway, for modes 1, 5 and 7, the same errors already explained occur.

Although this method is more accurate, for some numerical issues a failure of the computation can happen (modes 3 and 4). For this reason, all the results coming from the three different methods are reported in the GUI (Figure 2.5).

Also in this case, a graphical output is provided: it shows the original curve, the fitted one and the results of the computation, as shown in Figure 2.8.

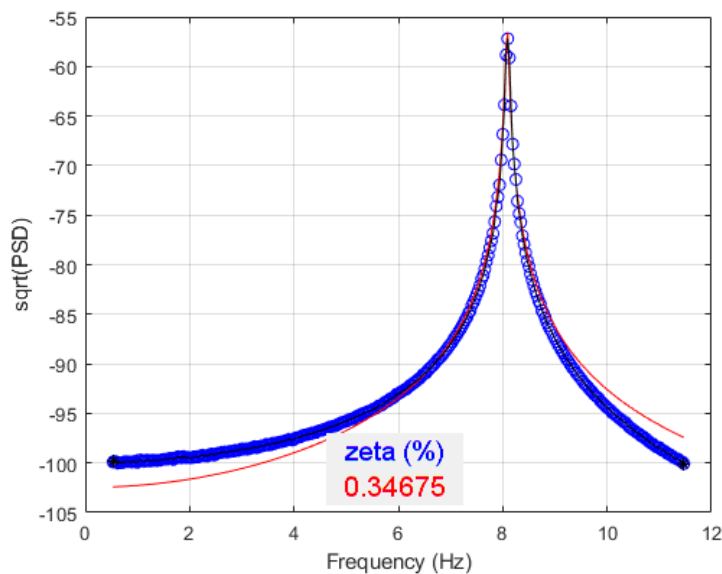


Figure 2.8: PSD fitting graphical output: in black the original curve and in red the fitted one. In this case (mode 1) they are almost superimposed.

2.4 MIMO systems

As already stated, a SIMO dataset can be obtained from more SISO ones by clicking on the button “Merge outputs”. It is also possible to obtain a MIMO dataset from more SIMO ones and this can be done by clicking on the button “Combine”. In this way the data are stored in a 3-D matrix, where the first dimension coincides with the number of outputs N_o , the second one with the number of inputs N_i and the third one with the number of samples of the analysed spectrum K , as shown in Figure 2.9.

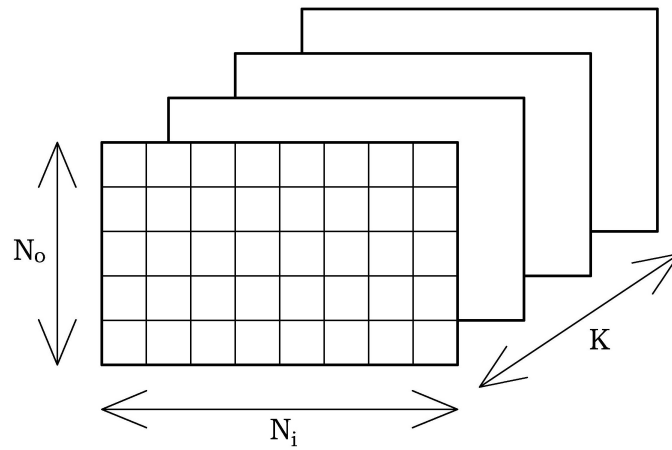


Figure 2.9: A simplified scheme of the 3D matrix.

Once a MIMO dataset is obtained, it is possible to click on “SVD-FRF” in order to perform the SVD and obtain the CMIF plot. The singular values are in this way saved in a matrix with N_{SV} rows and K columns.

In this case, on the plot more curves are present, as shown in Figure 2.10: they represent the different singular values obtained at each spectral line. This is exactly the case described in Chapter 1 and the *cross singular value or eigenvalue effect* may be noticed. For this reason the implementation of *vector tracking* is necessary: by following the highest singular value only, some points of the FRF may be neglected even if the MAC between the corresponding singular vector and the singular vector related to the singular value on the peak is higher than the minimum admissible MAC.

2.4.1 Vector tracking

Vector tracking starts when the analysis is started by clicking with the right mouse button.

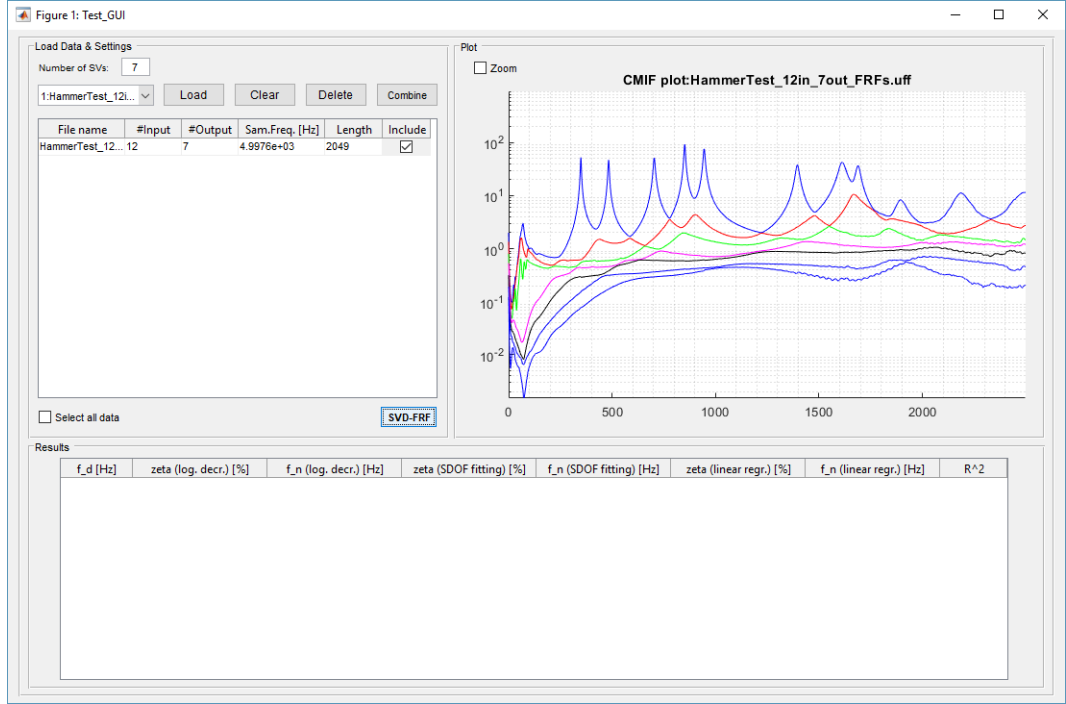


Figure 2.10: The GUI with the CMIF plot of a MIMO system.

First of all, the left singular vectors are stored in a matrix with $(N_{SV} \times N_o)$ rows and K columns, as shown in Figure 2.11, then the algorithm compares by means of Equation (2.1) the singular vector related to the picked singular value with all the singular vectors related to each the spectral line on both sides of the peak. This means that, at each iteration, N_{SV} MAC values are computed. The obtained MAC values are stored in a column of a matrix with N_{SV} rows and K column. At each iteration the maximum MAC is found among the last N_{SV} computed values and its row index is saved. The procedure goes on until all the last N_{SV} MAC values – that are related to a single spectral line – become lower than the minimum admissible MAC. This check can be easily implemented by verifying that the saved maximum MAC of the last iteration is lower than the threshold: if this is the case, also the other $N_{SV} - 1$ values will be lower than the minimum MAC, so the cycle is stopped, otherwise the next spectral line is considered.

Once the cycle is over on both sides of the peak, since the row indices of the maximum MAC values is saved, it is possible to pick the tracked singular values from the matrix that contains them all: at each spectral line, that corresponds to a column, the index of the maximum MAC indicates the row of the singular value that has to be chosen. The picked values are stored in a null vector with K elements and at this point the procedure is the equal to the one described in Paragraphs 2.2.2 and 2.2.3.

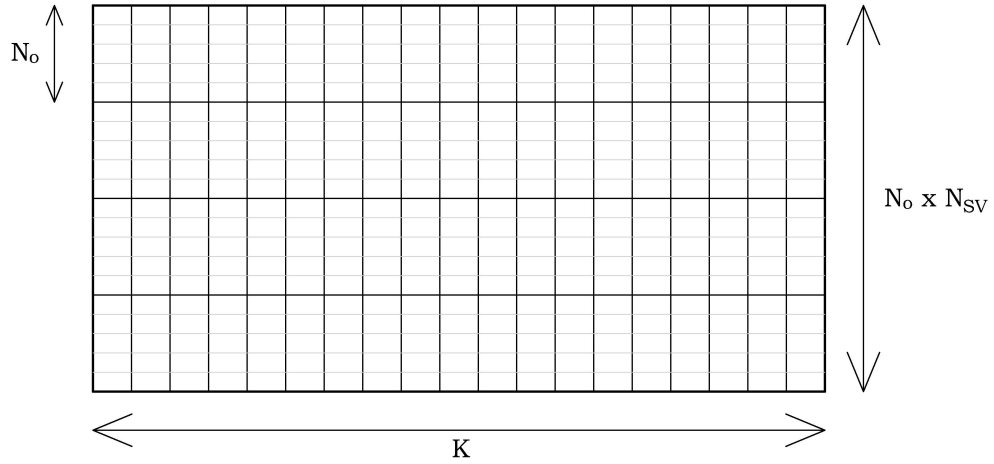


Figure 2.11: A simplified scheme of the matrix containing the singular vectors.

In Tables 2.4, 2.5 and 2.6 some experimental results are shown: they come from an impact test of an aluminium plate with 7 outputs and 12 impact points. The reference values have been computed with the RFP-Z method implemented in *ARTeMIS Modal*.

Mode	Natural frequency [Hz]		Damping ratio [%]		
	Reference	Experimental	Reference	Experimental	Δ [%]
1	66.97	69.67	8.414	5.908	29.78
2	349.06	348.96	0.599	0.567	5.33
3	483.22	483.17	0.572	0.554	3.23
4	704.10	704.02	0.629	0.633	0.56
5	851.36	851.64	0.386	0.398	3.03
6	945.62	945.60	0.475	0.499	5.09
7	1396.02	1395.8	0.667	0.588	11.89
8	1612.78	1611.9	1.058	1.411	33.40
9	1689.60	1688.7	0.677	0.736	8.74
10	1893.76	1893.6	1.354	0.619	54.28
11	2183.07	2185.3	1.590	0.851	46.46

Table 2.4: Summary of the results obtained by using the logarithmic decrement method (MIMO).

2.5 Symmetric structures

In presence of symmetric structures, it is very common to have resonance peaks also on the second singular value, at a frequency that is very close to one peak

Mode	Natural frequency [Hz]		Damping ratio [%]			R^2
	Reference	Experimental	Reference	Experimental	Δ [%]	
1	66.97	69.75	8.414	6.242	25.81	0.980
2	349.06	348.96	0.599	0.550	8.25	0.972
3	483.22	483.17	0.572	0.539	5.73	0.967
4	704.10	704.02	0.629	0.598	4.86	0.962
5	851.36	851.64	0.386	0.374	3.03	0.961
6	945.62	945.60	0.475	0.481	1.26	0.954
7	1396.02	1395.8	0.667	0.639	4.21	0.919
8	1612.78	1611.8	1.058	1.302	23.07	0.907
9	1689.60	1688.7	0.677	0.695	2.69	0.824
10	1893.76	1893.8	1.354	1.372	1.30	0.834
11	2183.07	2185.4	1.590	2.096	31.82	0.789

Table 2.5: Summary of the results obtained by using the linear fitting method (MIMO).

Mode	Natural frequency [Hz]		Damping ratio [%]		
	Reference	Experimental	Reference	Experimental	Δ [%]
1	66.97	69.81	8.414	8.682	3.18
2	349.06	348.96	0.599	0.600	0.12
3	483.22	483.17	0.572	0.571	0.16
4	704.10	704.02	0.629	0.642	1.99
5	851.36	851.64	0.386	0.400	3.58
6	945.62	945.60	0.475	0.516	8.72
7	1396.02	1395.8	0.667	0.670	0.49
8	1612.78	1611.9	1.058	1.096	3.56
9	1689.60	1688.7	0.677	0.720	6.37
10	1893.76	1893.8	1.354	1.433	5.83
11	2183.07	2185.5	1.590	1.684	5.29

Table 2.6: Summary of the results obtained by using the PSD fitting method (MIMO).

on the first singular value. In these cases, theoretically speaking, the two modes should be characterised by the same natural frequency and damping ratio, with equal mode shapes but 90° rotated. In practice, this condition is not so common, due to little asymmetries of the structure, that, for small and light structures, can be also caused by the accelerometers, that may not be placed in symmetric positions.

For this reason, the code has been modified in order to be able to pick also points on the second singular value.

2.6 C++ implementation

The written MATLAB code can not be directly included in *ARTEMIS Modal*, since the latter is written in C++ language.

For this reason, a new GUI-free script has been written: it receives as input the results of the SVD (already present in *ARTEMIS Modal*), asks the user to indicate the index of the point that corresponds to the peak to be investigated and the number of the singular value that peaks (just in case of more than one SV).

As output, it provides the damped frequency, the three different values of the damping ratios, the values of R^2 and the three values of the natural frequencies. For simple structures, such as beams or plates, the mode shape is also plotted on a static figure and in an animation.

The only difference from the GUI-based script is that a different graphical output is provided, in order to easily read the indices of the points. It consists of two CMIF plots: the first one has the frequency and the second one has the index on the horizontal axis, as shown in Figure 2.12.

Since this script is much simpler than the previous one, it represent the starting point for the C++ implementation, performed by the Structural Vibration Solutions A/S staff.

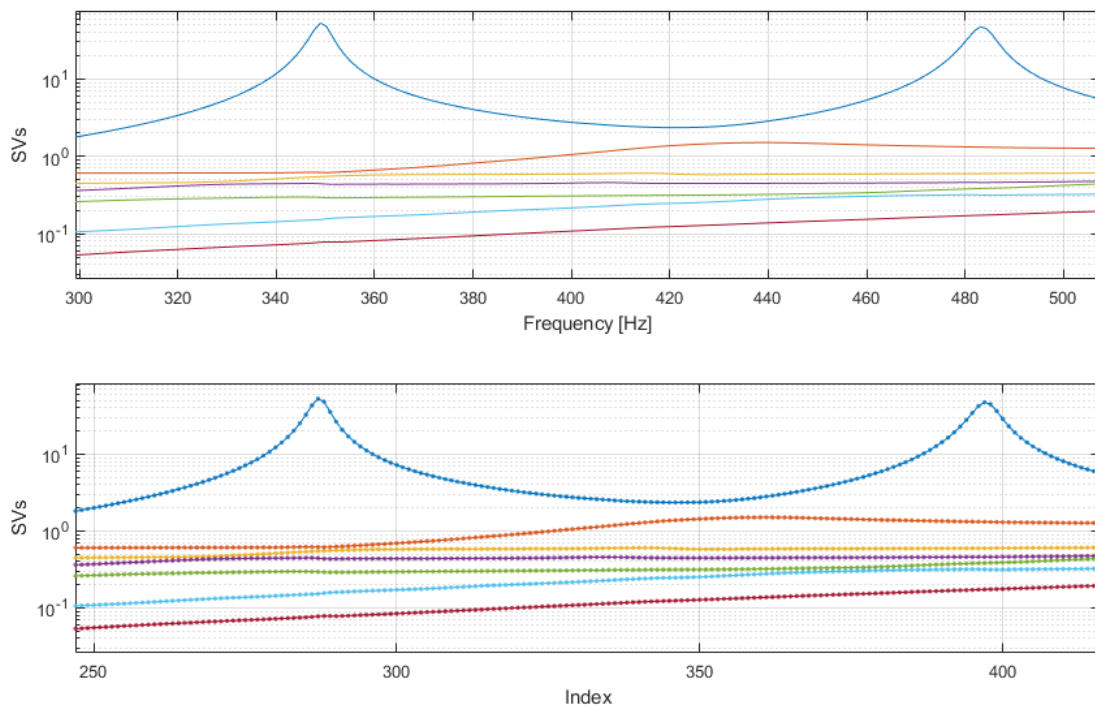


Figure 2.12: On the dotted plot MATLAB *datatips* can be used in order to read the index of the chosen point.

2.7 Automation of the procedure

In order to simplify the use of this program, a fully automatic version has been developed.

An automatic program is very convenient, especially for companies with inexperienced staff. In fact, with this kind of program it is sufficient to load the data obtained from the SVD, that is already implemented in *ARTEMIS Modal*, and start the computation: it gives as an output the results without any further intervention by the user.

Essentially, an automatic research of the peaks has been implemented and, once they are picked, the already explained computation starts, in order to obtain the damping ratios ζ_r and the damped frequencies $\omega_{d,r}$.

This search can be divided in different steps:

- 1) the Modal Coherence function is computed;
- 2) a threshold T is set in order to find the spectral lines where the peaks may be located and first check on them;
- 3) in each interval of spectral lines where a single mode is dominant, the maximum is found in the first singular value;
- 4) a second check is performed in order to discard maxima that don't correspond to a peak;
- 5) in the remaining intervals, the peaks in the second singular value are found;
- 6) the same check as before is performed in order to discard maxima that don't correspond to a peak in the second singular value;
- 7) further checks based on the MAC.

2.7.1 In-depth analysis

Modal Coherence

The so-called Modal Coherence is a function that will be close to one in the regions where a specific mode is dominating, which is around the resonance peaks, and will drop significantly between them, since the modes are mixed. Since it is a function of the frequency, it has as many points as the CMIF. For this reason it is particularly useful to plot it on the CMIF plot in order to visually recognise the

frequency intervals where the peaks are located.

It is computed in the following way: for each spectral line k , the function is computed by using the first left singular vectors by means of the equation below:

$$C_k = \frac{1}{2K} \sum_{\substack{i=-K \\ i \neq 0}}^K \{U\}_{k-i}^H \{U\}_k \quad (2.9)$$

where K is the number of the considered spectral lines on each side of the spectral line k . The function becomes smoother and smoother by increasing K [5].

Threshold setting

In order to identify the frequency intervals where the peaks may be located, a threshold T is set, at 0.8 for example. In this way, it has been possible to save the indices of the limits of the intervals where $C > T$, that may contain a resonance peak. Before the peaks research, intervals containing a few elements are discarded; the minimum number of elements is chosen by the user. This parameter can not be constant because, due to the obtained frequency resolution Δf , it is difficult to set a universally acceptable parameter.

Peaks search

In each remaining interval, the index of the local maximum of the first singular value is saved: it may correspond to a resonance peak.

Once a local maximum has been found in each interval, a check is needed in order to establish if that maximum is a peak or not.

For this reason, the routine checks that the maximum is at least higher than the interval limits plus a certain percentage, that can be adjusted in order to obtain good results. If this is not true, the interval and the maximum are discarded.

After this step, every frequency interval contains a resonance peak.

Second singular value

In this condition it is useful to check if the second singular value contains any peak, which is very common with symmetrical structures, as already explained. Since every possible peak in the second singular value appears below those of the first singular value, the previously detected intervals are used.

Again, in each interval the local maximum is found and it is checked that it is higher than the interval limits plus a certain percentage.

Further checks

Once all the actual resonance peaks have been found on both singular values, two MAC-based checks are performed. For both of them, the left singular vectors $\{U\}$ are used. The SVD produces, for each spectral line, a left singular vector for each singular value: by using the same indices that point to the resonance peaks, it is possible to associate a singular vector to each mode.

The first one concerns the couples of sibling modes that occur on the two singular values at the same frequency: the MAC between them is calculated and if it is higher than 0.3 the mode on the second singular value is discarded. It's important to remark that the frequencies of two sibling modes may be slightly different due to small asymmetries of the structure and that, for small and light structures, these asymmetries may be also caused by the accelerometers, if they are not placed in symmetric positions.

The second one is based on the MAC matrix and so the matrix needs to be built.

At first, all the detected mode indices are stored in a vector and sorted in increasing order, then a vector with the same length is built and each of its elements indicates if the corresponding mode belongs to the first or the second singular value: if the element is equal to 0, the mode belongs to the first singular value and if it is equal to 1 the mode belongs to the second one. This step is fundamental in order to pick the right singular vector for each mode.

Once this information is known, the MAC matrix can be built. The expected result is a matrix containing values close to 1 (or anyway greater than 0.9) on the main diagonal and values close to 0 (or anyway lower than 0.3) out of it. For different reasons, especially with close-spaced modes, it can happen that high MAC values appear on the first diagonals above and below the main one, due to some similarities between the two modes. In this cases, one of the two modes often shows a higher complexity than the other one.

In order to solve this problem, the two modes are further investigated: the elements of the two corresponding rows are summed up in order to understand which mode is more correlated to all the others. Then, the mode that has this characteristic is eliminated and all the vectors containing the intervals limits and the indices of the resonance peaks are updated. A new MAC matrix is also built.

Damping computation

At this point, all the indices of the resonance peaks are given as input to the previously described routine in order to compute the damping ratios ζ_r and the damped frequencies $\omega_{d,r}$.

Graphical output

With this automatic procedure, the graphical output shown in Figure 2.12 is nomore useful and for this reason is not provided. At its place, besides the plots shown in Figures 2.6 and 2.8, three additional graphical outputs are provided: the CMIF plot with the Modal Coherence function superimposed, the MAC matrix and the updated MAC matrix after the correction, if necessary.

Figures 2.13 and 2.14 have been obtained by analysing the rectangular aluminium plate with 7 output channels and 12 impact points with a sampling frequency $f_s = 5000 \text{ Hz}$.

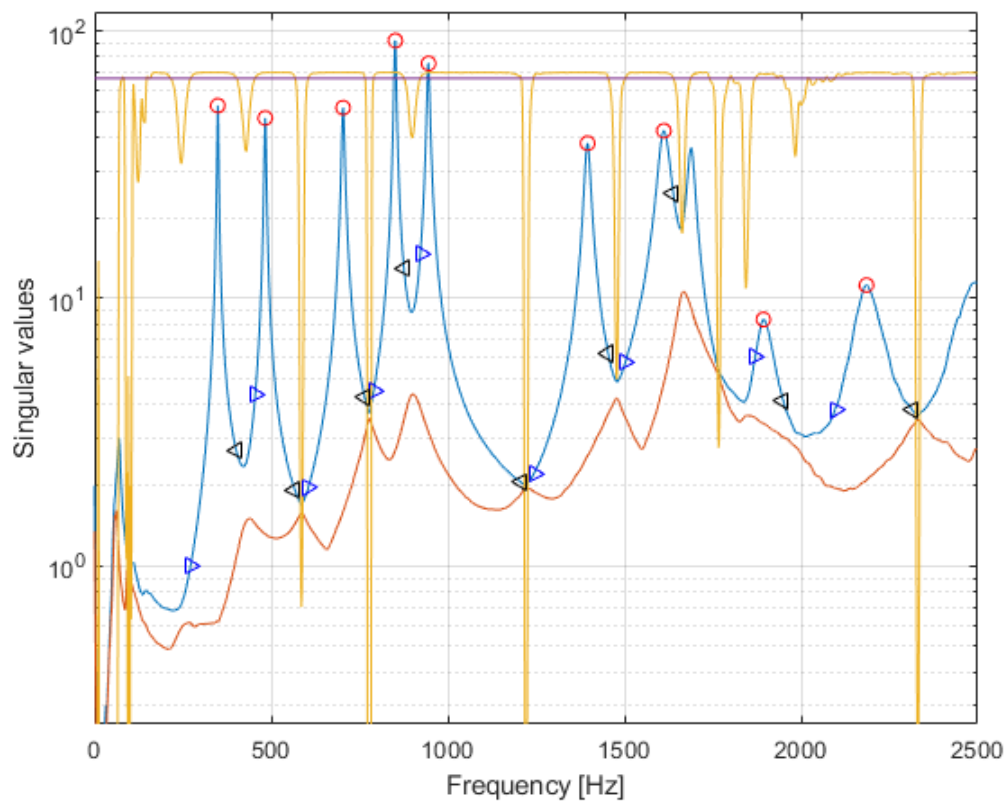


Figure 2.13: CMIF plot with Modal Coherence: threshold, intervals limits and peaks are highlighted.

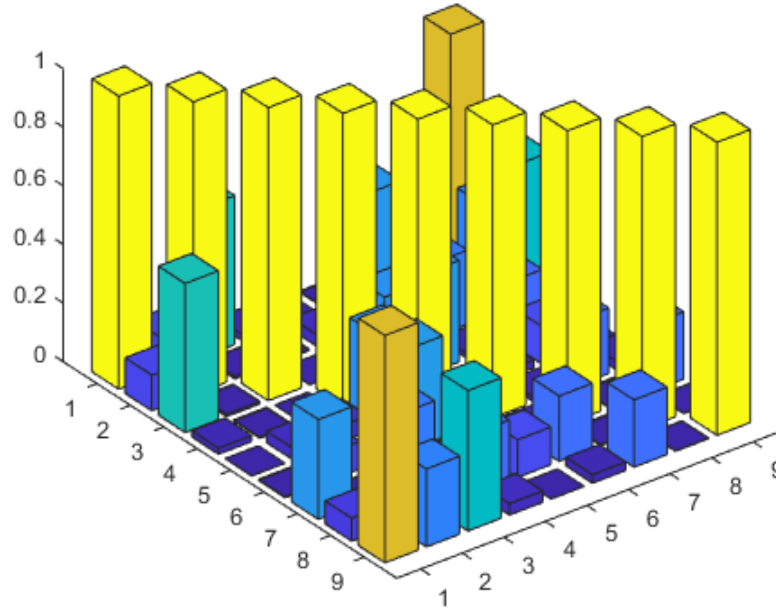


Figure 2.14: MAC matrix of the aluminium plate with 12 input and 7 output channels.

2.7.2 Mode shapes plots

In this script, a graphical visualisation of the mode shapes is also provided for simple structures, such as beams and plates. They are plotted in a static picture and in a video animation.

In order to plot the mode shapes, the response coming from all the points of the grid are necessary and it is sufficient to excite the structure just by means of a couple of impact points. After building the MIMO dataset and the CMIF plot, the mode shapes can be plotted.

It is important to remark that the mode shapes $\{\psi_r\}$ are estimated by the left singular vectors $\{U_k\}$, where k corresponds to the index of the spectral line that coincides with the peak of mode r . Since the vectors $\{U_k\}$ are usually complex, it has been necessary to compute the correspondent real vectors by means of the following equation, applied to each component:

$$\psi_{r,i} = |U_{k,i}| \cos [\angle(U_{k,i})] \quad (2.10)$$

This operation is necessary because in complex mode shapes the absolute value of each component gives the maximum displacement amplitude of the correspondent DOF and their phases give the delay between the moments in which the different DOFs reach the maximum displacement.

2.8 Testing

The method has been verified with different structures and conditions, in order to define the limits of its reliability, with both numerical and experimental tests.

The numerical tests have been carried out on a lumped parameters model and a continuous one, built by using a FE (**F**inite **E**lement) approach, that gives the opportunity of building a large variety of different structures. In order to build the FE model, ANSYS Mechanical APDL has been used.

Before running the analysis of the numerical lumped parameters systems, three MATLAB scripts have been used: the first one builds the mass $[M]$, the damping $[C]$ and the stiffness $[K]$ matrices of the system [2], the second one computes the FRFs with the hypothesis of proportional viscous damping [6] and the third one is the GUI-based one described in the first part of this Chapter, that builds a MIMO dataset from many SISO ones and computes the CMIF. Some random noise has been added to the FRFs in order to get a little closer to a real experiment. The same workflow has been followed for the FE model, even if the second script has been slightly modified in order to select the right DOF of the system.

The script used in order to compute the SISO FRFs of the numerical systems computes the receptance α_{pq} between the input point q and the output point p in the form:

$$\alpha_{pq}(\omega) = \sum_{r=1}^n \frac{\phi_{pr}\phi_{qr}}{\omega_r^2 - \omega^2 + i(2\zeta_r\omega_r)} \quad (2.11)$$

where $\{\phi_r\}$ is the modal mass scaled eigenvector:

$$\{\phi_r\} = \frac{\{\psi_r\}}{\sqrt{m_r}} \quad (2.12)$$

It's important to remark that this scaling operation is not necessary in MATLAB, since the command `[phi,lam]=eig(K,M)` produces modal mass scaled eigenvectors. Once the receptance is computed, the inertance $H(\omega)$ is calculate by multiplying it by $-\omega^2$:

$$H_{pq}(\omega) = -\omega^2 \cdot \alpha_{pq}(\omega) \quad (2.13)$$

The real system is a rectangular steel plate, tested with different numbers of input and output channels by using the Data Acquisition module available in *ARTEMIS Modal*.

The experimental hardware is composed by:

- 1) 1 National Instruments model NI cDAQ-9172 chassis;
- 2) 2 National Instruments model NI 9233 input modules with the following charac-

teristics:

- 4 simultaneous analog input channels;
 - 24-bits Delta - Sigma ADC;
 - $\pm 5 V$ input range.
- 3) 1 PCB Piezotronics model PCB 086C01 Modally Tuned impact hammer;
 - 4) 7 Brüel & Kjær monoaxial accelerometers.

The results of all the tests show that the method is more accurate when many output channels are used (the number of impact points also affects the results, but this is true for every method; for this reason this number is usually large). This behaviour was predictable: in both the automatic search of peaks and in the definition of the frequency intervals where a mode is dominant, the Modal Assurance Criterion is widely used. It involves the left singular vectors $\{U_k\}$, so, in order to have many components, it is convenient to have many accelerometers. In fact, the number of components of the left singular vectors is always equal to the number of output channels.

For the sake of completeness some results are shown.

2.8.1 Lumped parameters numerical system

The 15 degrees of freedom lumped parameters numerical system in Figure 2.15 has been generated. The FRF have been computed for different cases:

- 1) 15 impact points and 15 output channels (in this way the whole FRF matrix is obtained);
- 2) 15 impact points and 8 output channels (DOFs 1, 3, 5, 7, 9, 11, 13 and 15);
- 3) 15 impact points and 4 output channels (DOFs 1, 2, 3 and 4);
- 4) 15 impact points and 2 output channels (DOFs 1 and 7).

By reducing the number of output channels, the results became less clear and less complete: in a structure like this 15 modes should be found, but even the first case, that is the ideal situation, only 12 of them appear. This happens because, in the automatic procedure, only the first and the second singular values are investigated and the last three modes are located on singular values lower than the second. The choice of investigating just the first two singular values comes from the fact that in real cases it is quite uncommon to have peaks on lower ones. Anyway, it is always possible to analyse the last 3 modes by using the manual procedure.

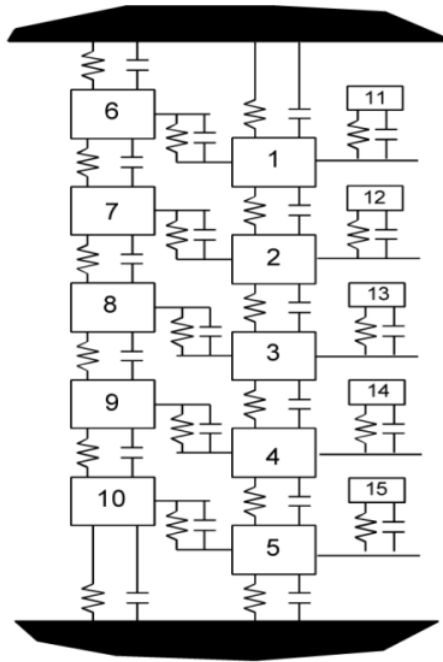


Figure 2.15: 15 DOFs numerical system scheme [2].

Case 1) In this case, all the DOFs are excited and measured, so 225 SISO FRFs have been generated. Then, they have been collected in groups of 15 in order to obtain 15 SIMO dataset with 1 input and 15 output channels. After that, they have been combined in order to obtain a MIMO dataset with 15 input and output channels.

In Table 2.7 the results coming from the PSD fitting method are shown. The reference data are the exact ones, since the system is numerical. As regards the damping ratios, except for mode 1, all the values have a relative error lower than 3%, that is a very good result; ζ_1 shows an error equal to almost 55%, but it can be justified by the low value of the damping ratio itself and of the natural frequency: it is quite normal, in fact, to have some bad data at low frequencies. As regards the natural frequencies, the results are practically exact, thanks to the high number of singular values and to the good obtained damping ratios.

Figures 2.16 and 2.17 show the graphical outputs coming from the same computation. In the first one the 12 automatically detected modes can be appreciated. They come from both the singular values and, as it can be noticed, all the false peaks generated by the *crossing singular value or eigenvalue effect* are not taken into account. In the second one the MAC matrix shows that the results are acceptable, since there isn't any high value out of the main diagonal, especially in the diagonals above and below the main one.

Case 4) In this case 15 DOFs are excited but just two of them are measured (DOFs 1 and 7): from Figure 2.19 it can be easily noticed that the results are much more

Mode	Natural frequency [Hz]			Damping ratio [%]		
	Reference	Experimental	Δ [%]	Reference	Experimental	Δ [%]
1	15.99	15.98	0.04	1.004	0.455	54.70
2	30.86	30.85	0.06	1.937	1.974	1.90
3	43.61	43.62	0.02	2.734	2.746	0.43
4	46.47	46.50	0.07	2.913	2.923	0.35
5	53.36	53.34	0.03	3.339	3.390	1.51
6	53.42	53.46	0.07	3.345	3.332	0.39
7	59.46	59.41	0.10	3.716	3.811	2.54
8	61.65	61.67	0.02	3.855	3.838	0.44
9	68.89	68.87	0.02	4.301	4.311	0.24
10	73.73	73.66	0.09	4.596	4.646	1.09
11	143.54	143.65	0.08	2.278	2.271	0.31
12	143.68	143.79	0.08	2.296	2.277	0.81
13	143.88	144.01	0.09	2.324	2.311	0.54
14	144.11	144.25	0.10	2.357	2.336	0.93
15	144.30	144.43	0.09	2.386	2.360	1.08

Table 2.7: 15 DOFs system results with 15 input and output channels.

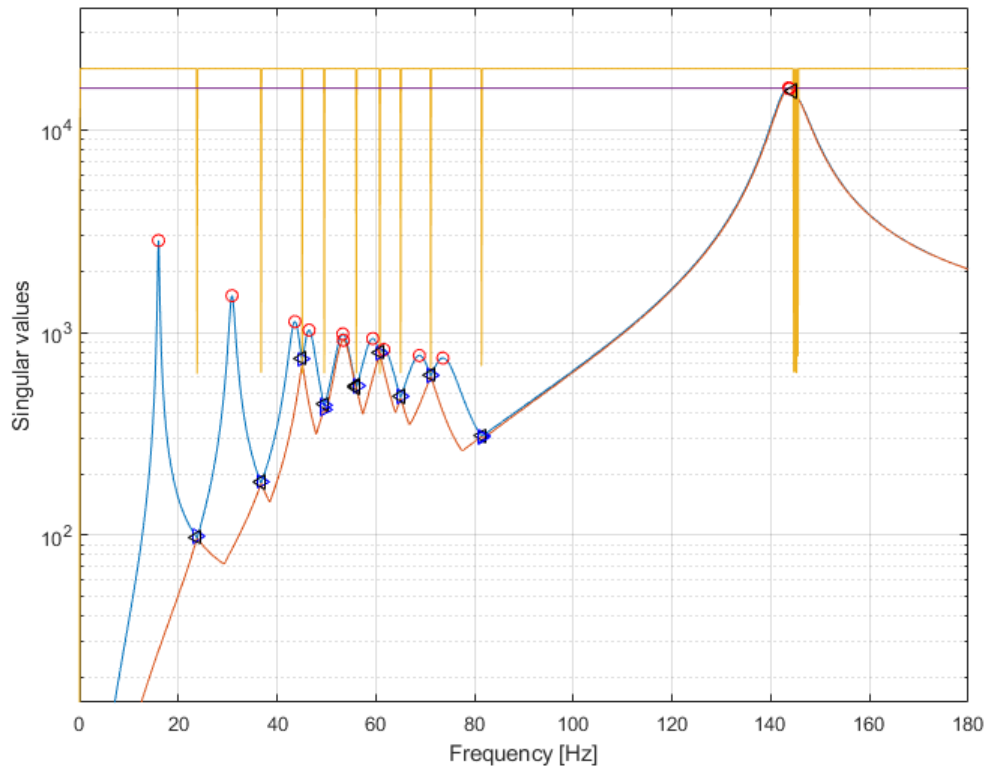


Figure 2.16: CMIF plot with Modal Coherence of the 15 DOFs system with 15 input and output channels.

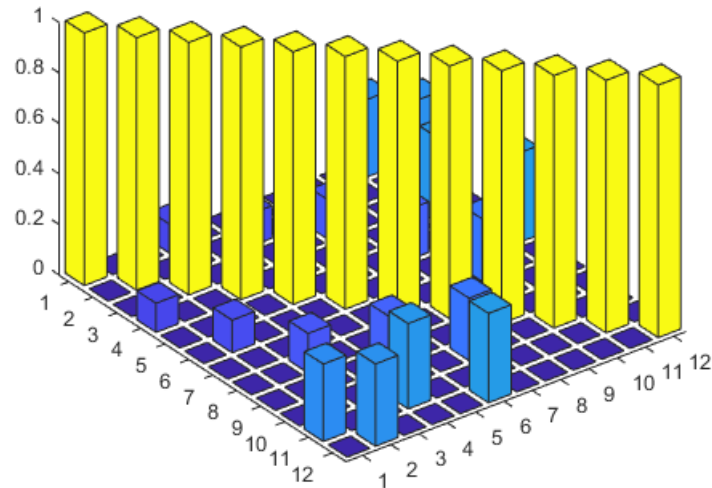
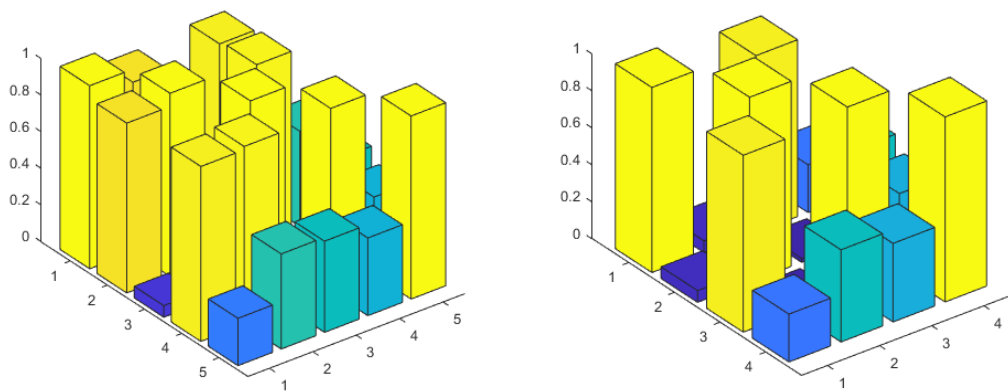


Figure 2.17: MAC matrix of the 15 DOFs system with 15 input and output channels.

confused.

In first instance, all the information are carried by two singular values instead of fifteen and this brings to a bad CMIF plot, that leads to a bad identification of modal parameters. Then, the left singular vectors are made by just two components and this brings to a worse Modal Coherence function and to a bad MAC matrix. Due to this last issue, as it can be noticed from Figures 2.18 and 2.19, mode 2 is discarded because it appears to be highly correlated to mode 1. In case 1), when this issue does not occur, modes 1 and 2 don't seem to be correlated at all.



(a) The couple (1, 2) shows a high MAC value.

(b) Mode 2 has been discarded (see Figure 2.19).

Figure 2.18: MAC matrix before and after the last check.

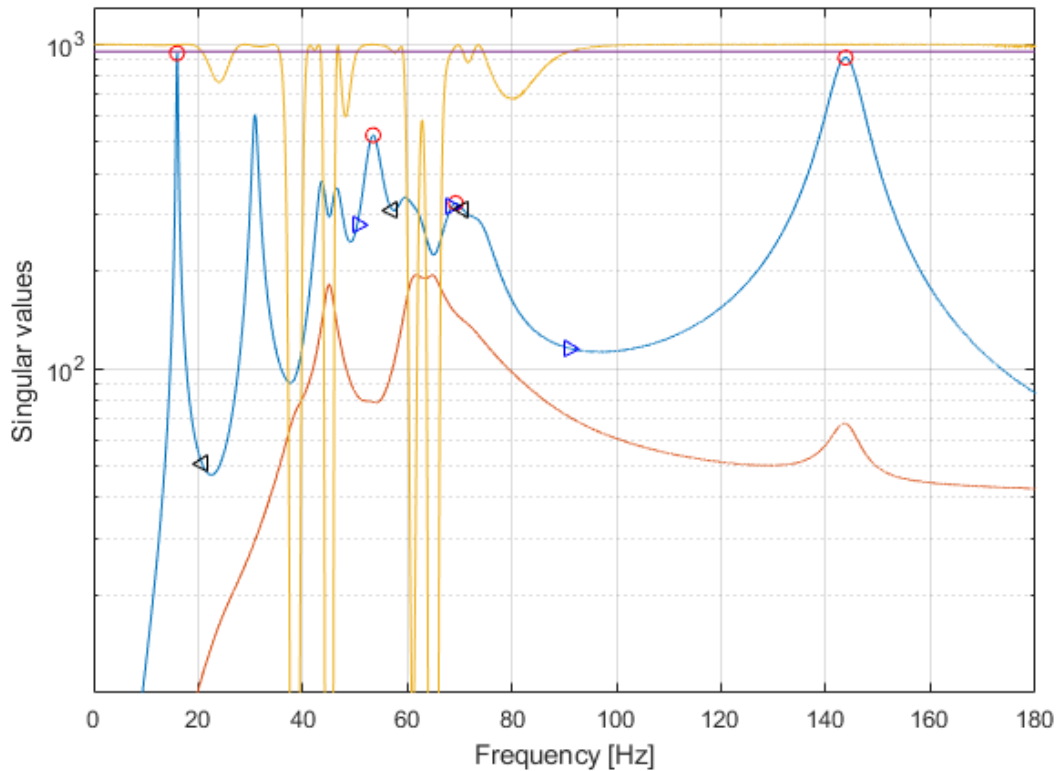


Figure 2.19: CMIF plot with Modal Coherence of the 15 DOFs system with 15 input channels and 2 output channels: only 4 out of 15 modes have been detected.

2.8.2 Continuous numerical system

As already explained, a continuous numerical system has been analysed as well.

By using ANSYS Mechanical APDL a free-free steel plate with the same dimensions as the real one that will be analysed in Paragraph 2.8.3 has been generated.

It has been subdivided in 24 elements, in accordance with the grid used in the test on the real plate. The model has been constructed by using solid elements (SOLID45) with 8 nodes per element. Each node has three DOFs, u_x , u_y and u_z , so, having 70 nodes, the whole model has 210 DOFs. It is shown in Figure 2.20.

After building the model, the modal analysis has been performed. It's important to remark that ANSYS gives the opportunity to choose how many modes have to be taken into account during the computation. In this case, since the model is little and simple, 50 modes have been considered.

In order to extract the mass $[M]$ and the stiffness $[K]$ matrices of the system, all the considered modes must be expanded through the `MXPAND` command.

ANSYS gives also the opportunity to choose the type of mass matrix to use for the analysis (lumped or consistent): a consistent mass matrix has been used.

The results, like natural frequencies and modal participation factors for the three direc-

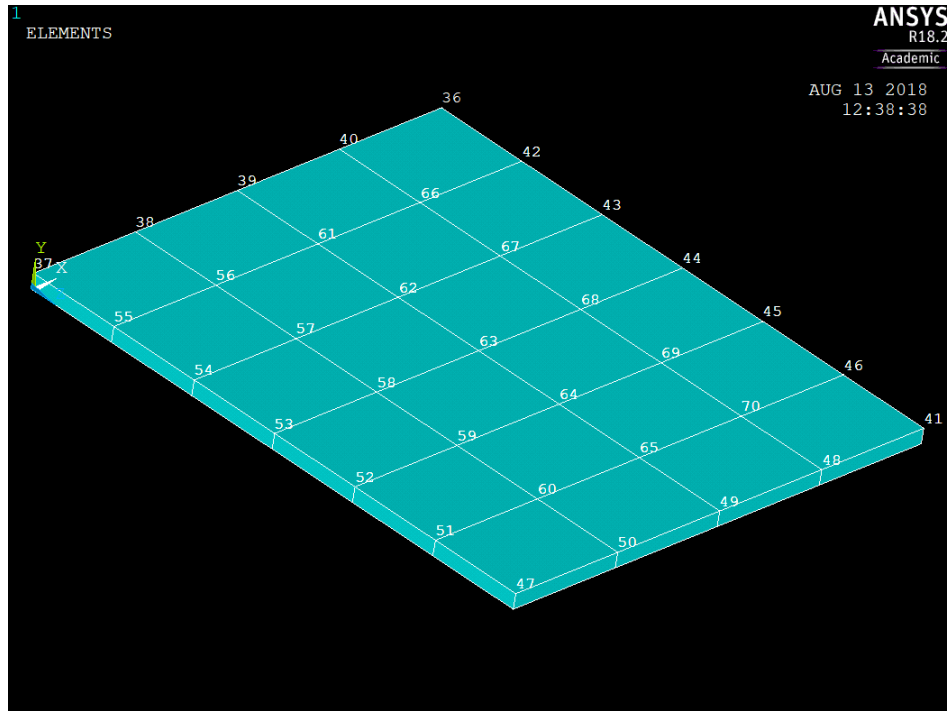


Figure 2.20: FE model with node numbers.

tions, have been saved in a *.txt file, that contains also all the characteristics of the model.

After the analysis, the matrices have been exported, in addition to a *mapping* file which will be useful later. The ANSYS command used to perform these operations is HBMAT, available in the /AUX2 post processor, that gives the opportunity to read the automatically generated *.full file and to export in two different ASCII files (*.matrix) the mass and the stiffness matrix.

These two files have been imported in MATLAB by using a script provided by Structural Vibration Solutions A/S staff, that reads the *.matrix files and saves the data in two sparse matrices in MATLAB workspace.

Known $[M]$ and $[K]$, it is possible to build a proportional viscous damping matrix:

$$[C]_p = \alpha[M] + \beta[K] \quad (2.14)$$

The same matrix can also be built within ANSYS, by setting the coefficients α and β as material properties with the command MP, just like the Young modulus E , and by exporting it with the HBMAT command, but this method has not been used because it is much quicker to change the coefficients in MATLAB without importing the three matrices every time a modification of the parameters is required.

Since, as already said, the model has 210 DOFs, the three matrices have 210 rows and columns.

Once all the matrices are available, the modal approach can be used to decouple the

210 equations: using the MATLAB command `eig`, it is possible to compute eigenvalues and eigenvectors. By using the well known relations below, it is possible to obtain the natural frequencies and the diagonal modal matrices:

$$f_r = \frac{\sqrt{\lambda_r}}{2\pi} \quad (2.15)$$

$$[\bar{M}] = [\Psi_r]^T [M] [\Psi_r]$$

$$[\bar{C}] = [\Psi_r]^T [C] [\Psi_r]$$

$$[\bar{K}] = [\Psi_r]^T [K] [\Psi_r]$$

At this point, in order to check that all the process has been carried out properly, first of all it has been noticed that the first six natural frequencies are null, since they correspond to the six rigid body motions, and then the computed natural frequencies have been compared to those contained in the results file generated in ANSYS: the outcome was positive.

Known all the modal damping terms \bar{c}_r , that can be read on the main diagonal of $[\bar{C}]$, it is possible to compute the modal damping ratio associated to each mode:

$$\zeta_r = \frac{\bar{c}_r}{2\sqrt{\bar{k}_r \bar{m}_r}} \quad (2.16)$$

These damping ratios, in addition to the natural frequencies computed by means of Equation (2.15), have been considered as reference parameters for the computation.

As already said, some operations have been necessary in order to refer to the right DOF of the FE model. It is necessary to use the *mapping* file: in the matrices exported from ANSYS, the order of the rows does not follow the order of the nodes. For example, it is not necessarily true that rows from 1 to 3 and from 4 to 6 refer to u_x , u_y and u_z related to node 1 and 2 and so on. The *mapping* file contains the relation between rows, nodes and DOFs, so it can be used in order to automatically convert the node number into the row number, specifying which DOF has to be taken into account. An extract of this file is shown:

Matrix	Eqn	Node	DOF
	1	5	UX
	2	5	UY
	3	5	UZ
	4	31	UX
	5	31	UY
	6	31	UZ
	⋮	⋮	⋮

Then, the FRFs can be plotted if needed, saved and loaded in the GUI-based program described in the first Paragraphs of this Chapter in order to compute the CMIFs. Once the CMIFs are computed and saved, the automatic program can be run. The FE model has been tested in different conditions:

- 1) low damping ($\alpha = 10^{-4}$, $\beta = 10^{-6}$);
- 2) medium damping ($\alpha = 2 \cdot 10^{-4}$, $\beta = 8 \cdot 10^{-6}$);
- 3) high damping ($\alpha = 4 \cdot 10^{-4}$, $\beta = 1.6 \cdot 10^{-5}$);

In this case, all the tests have been carried out using 35 impact points and 7 output channels. Even in this case, some random noise has been added in order to simulate a more realistic situation.

Case 1) Table 2.8 shows the results coming from the PSD fitting method.

The computed values for the natural frequencies and for the damping ratios can be considered fully acceptable. As regards mode 5, it has been detected by the automatic procedure, but then it has been discarded because it appears to be highly correlated to mode 6, as it can be seen in Figure 2.22. This is actually wrong, because these two modes have not close natural frequencies and have different mode shapes (Figures 2.28 form (a) to (d)). This error can be probably avoided by using more output channels. As regards mode 7, it has not been detected by the automatic procedure because it is very close to mode 8 and this causes problems in the Modal Coherence. For these reasons, both modes 5 and 7 have been picked manually. Figures 2.21 and 2.22 show respectively the resulting CMIF plot and the MAC matrix.

Mode	Natural frequency [Hz]			Damping ratio [%]		
	Reference	Computed	Δ [%]	Reference	Computed	Δ [%]
1	367.34	367.50	0.04	0.115	0.120	3.64
2	485.20	485.00	0.04	0.152	0.156	2.46
3	779.41	779.50	0.01	0.245	0.253	3.45
4	1027.47	1027.51	0.00	0.323	0.327	1.20
5	1201.04	1201.01	0.00	0.377	0.407	7.93
6	1586.39	1586.52	0.01	0.498	0.519	4.14
7	2398.67	2398.57	0.00	0.754	0.758	0.61
8	2430.80	2431.06	0.01	0.764	0.700	8.37

Table 2.8: FE model (low damping) results.

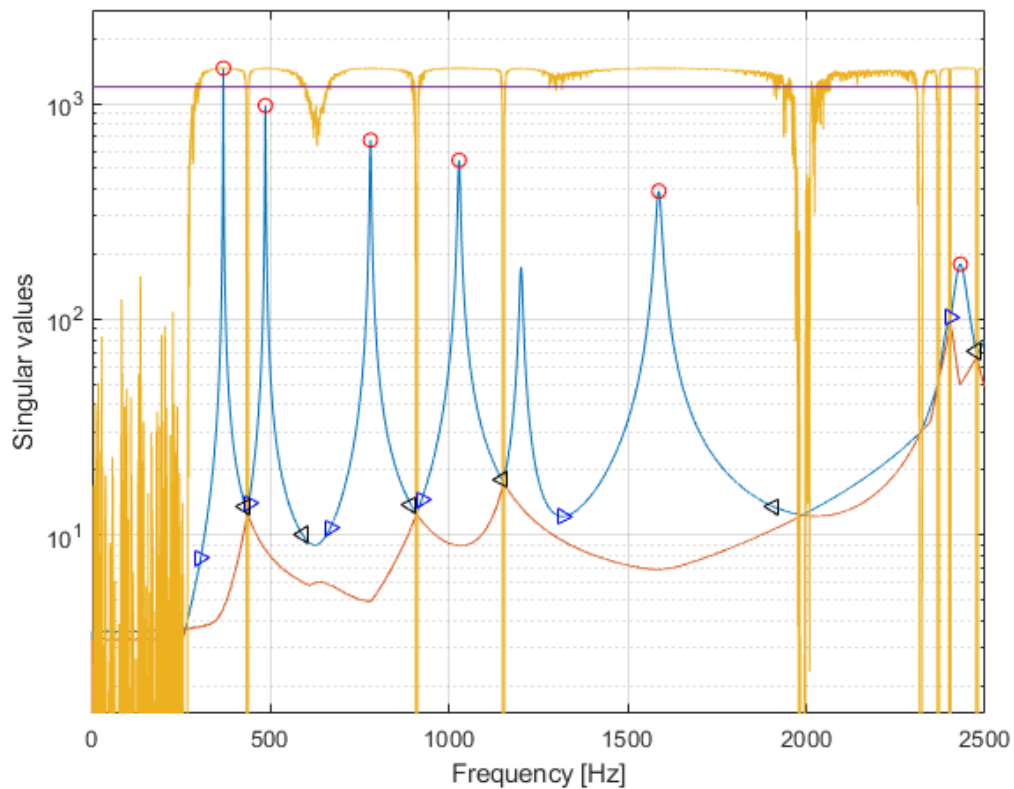
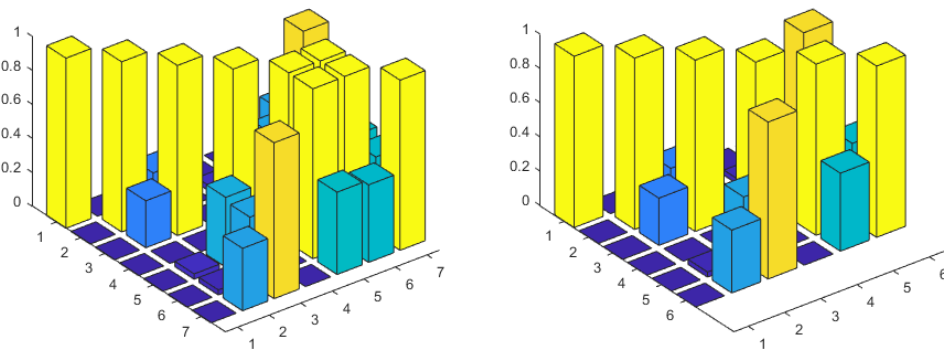


Figure 2.21: CMIF plot with Modal Coherence of the FE model (low damping): 6 out of 8 modes have been automatically detected.



(a) Modes 5 and 6 are highly correlated. (b) Mode 5 has been discarded (see Figure 2.21).

Figure 2.22: MAC matrix before and after the last check.

Case 2) Table 2.9 shows the results coming from the PSD fitting method. Also in this case, the computed values for the natural frequencies and for the damping ratios can be considered fully acceptable. As regards mode 5, all the considerations made in **Case 1)** are still valid, so it has been picked manually. Figures 2.23 and 2.24 show respectively the resulting CMIF plot and the MAC matrix.

Figure 2.23 shows also that modes 7 and 8 are practically absent due to the higher damping value and for these reason they can not be detected nor manually picked.

Mode	Natural frequency [Hz]			Damping ratio [%]		
	Reference	Computed	Δ [%]	Reference	Computed	Δ [%]
1	367.34	367.52	0.05	0.923	0.961	3.64
2	485.20	485.54	0.07	1.219	1.253	2.46
3	779.41	779.66	0.03	1.959	2.034	3.45
4	1027.47	1028.35	0.09	2.582	2.620	1.20
5	1201.04	1201.18	0.01	3.019	3.366	7.93
6	1586.39	1589.40	0.19	3.987	4.194	4.14
7	2398.67	-	-	6.029	-	0.61
8	2430.80	-	-	6.109	-	8.37

Table 2.9: FE model (medium damping) results.

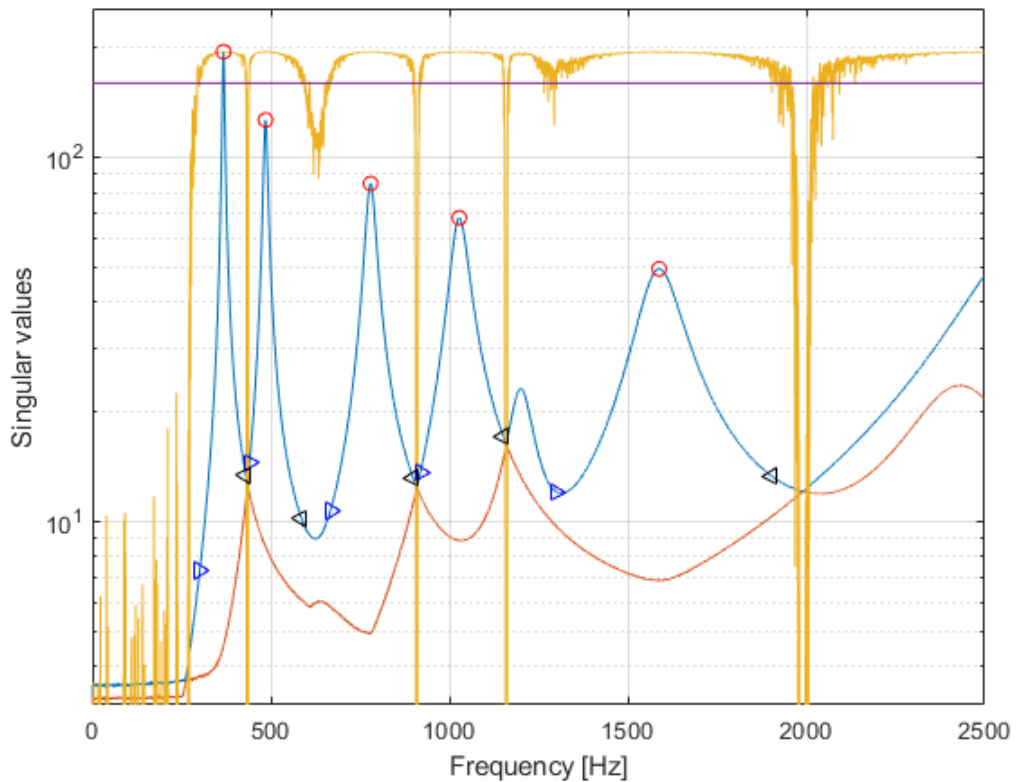
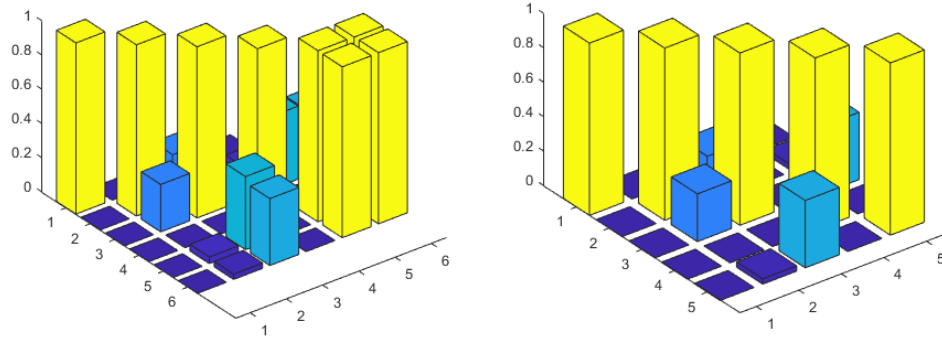


Figure 2.23: CMIF plot with Modal Coherence of the FE model (medium damping): 6 out of 8 modes have been automatically detected.



(a) Modes 5 and 6 are highly correlated. (b) Mode 5 has been discarded (see Figure 2.23).

Figure 2.24: MAC matrix before and after the last check.

Case 3) Table 2.10 shows the results coming from the PSD fitting method. The computed values for the natural frequencies and for the damping ratios can be considered fully acceptable, except for mode 5, that has been picked manually. Such a big error in mode 5 occurs because the peak is very low and smooth due to damping and because it is very close to an intersection between the first and the second singular values, that causes low values of the Modal Coherence function, as it can be seen in Figure 2.25. The low amplitude of the peak caused also a failure of the PSD fitting method and for this reason the reported value comes from the logarithmic decrement one. In the same Figure, it can be noticed that modes 7 and 8 are practically absent due to damping, like **Case 2**). Figure 2.26 shows the resulting MAC matrix.

Mode	Natural frequency [Hz]			Damping ratio [%]		
	Reference	Computed	Δ [%]	Reference	Computed	Δ [%]
1	367.34	367.57	0.06	1.846	1.926	4.30
2	485.20	485.65	0.09	2.439	2.511	2.96
3	779.41	780.65	0.16	3.918	4.094	4.49
4	1027.47	1032.43	0.48	5.165	5.265	1.95
5	1201.04	1204.26	0.27	6.037	2.070	65.71
6	1586.39	1599.90	0.85	7.974	8.579	7.59
7	2398.67	-	-	12.057	-	-
8	2430.80	-	-	12.219	-	-

Table 2.10: FE model (high damping) results.

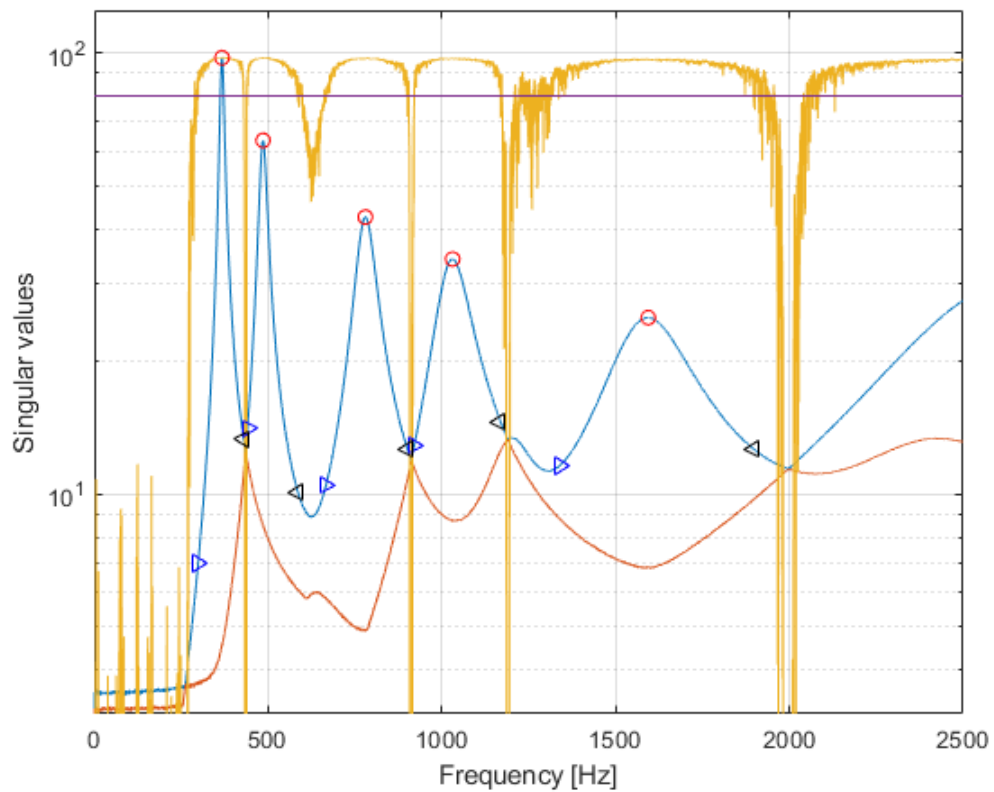


Figure 2.25: CMIF plot with Modal Coherence of the FE model (high damping): 5 out of 8 modes have been automatically detected.

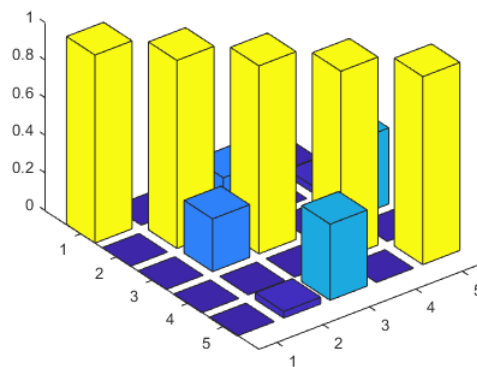


Figure 2.26: MAC matrix .

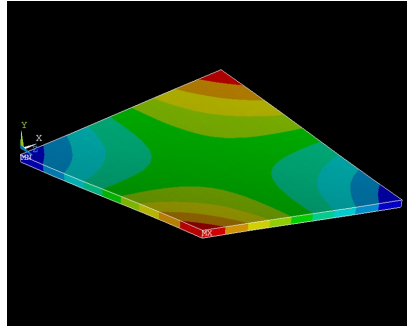
Mode shapes

When a modal analysis is performed in ANSYS, in addition to the natural frequencies and the modal participation factors, the mode shapes are available. For this reason a comparison between these mode shapes and those estimated in MATLAB has been carried out.

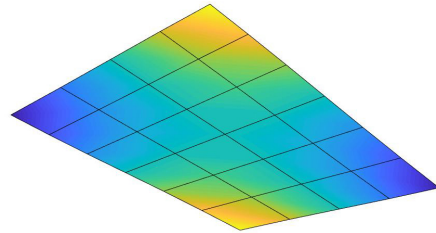
As already explained, in order to plot the mode shapes, all the points of the grid have to be measured. In this way the left singular vectors $\{U_k\}$ have 35 components. Once

the peaks have been detected, these components have been stored in a 7-by-5 matrix, in order to reconstruct the grid and easily plot the mode shapes.

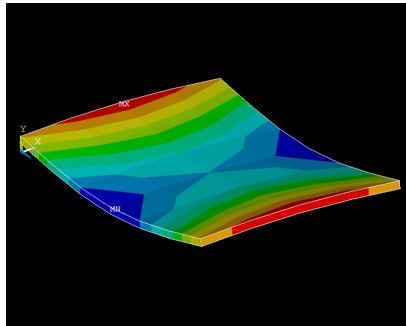
The mode shapes coming from ANSYS and MATLAB are here showed.



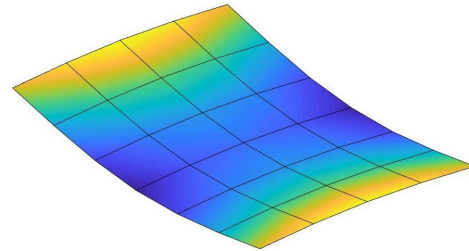
(a) ANSYS



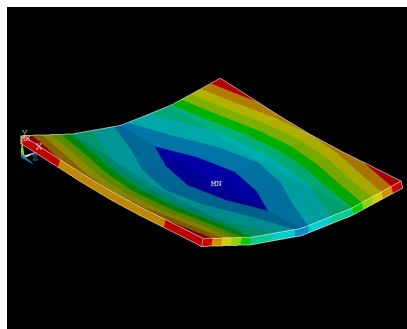
(b) MATLAB



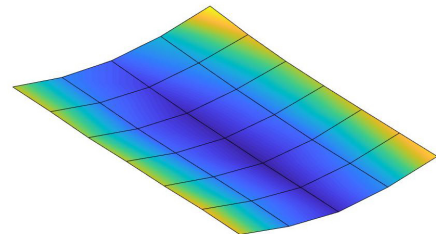
(c) ANSYS



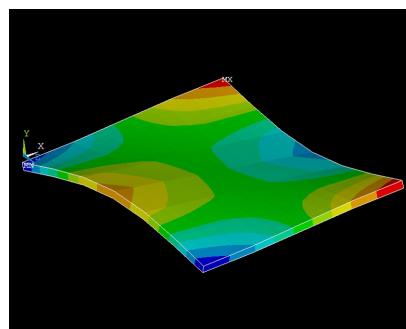
(d) MATLAB



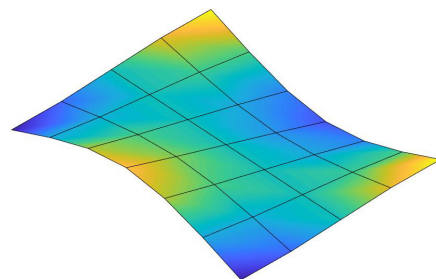
(e) ANSYS



(f) MATLAB

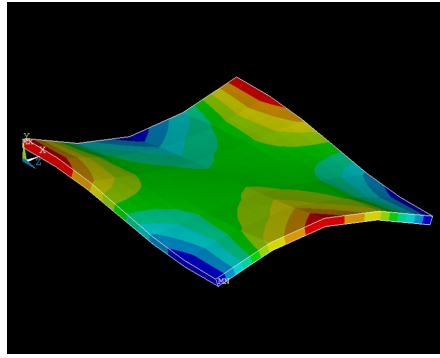


(g) ANSYS

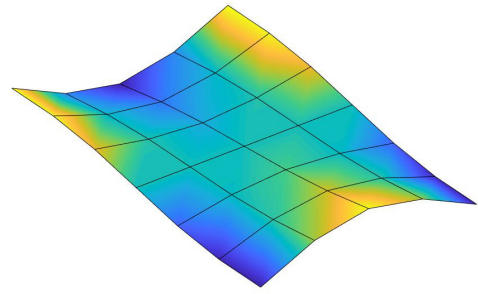


(h) MATLAB

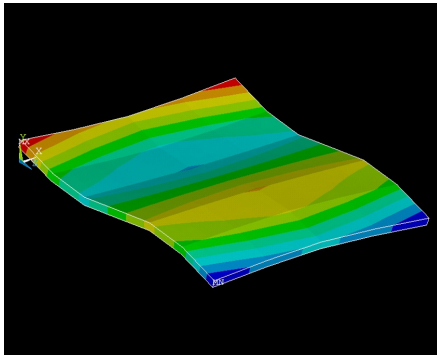
Figure 2.27: Modes 1 to 4.



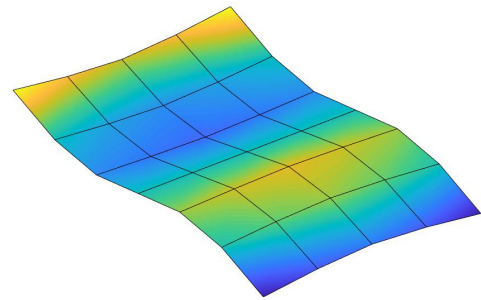
(a) ANSYS



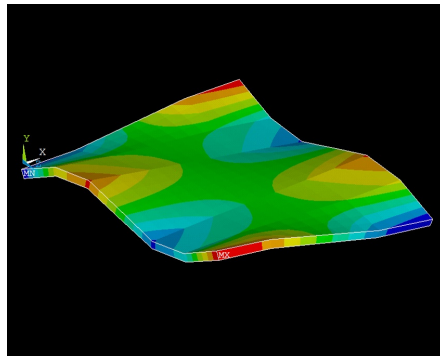
(b) MATLAB



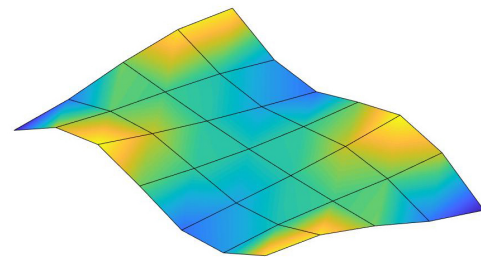
(c) ANSYS



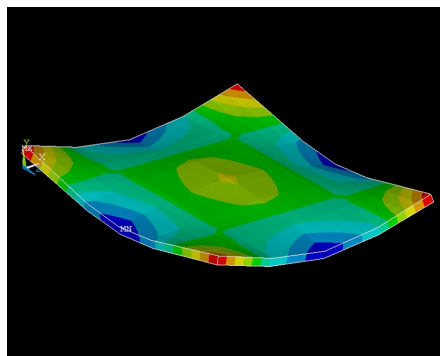
(d) MATLAB



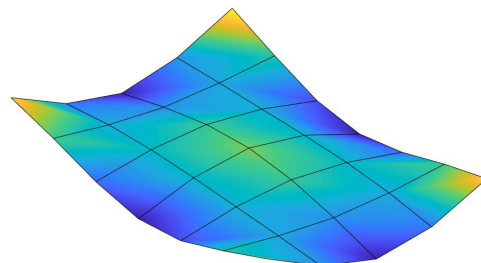
(e) ANSYS



(f) MATLAB



(g) ANSYS



(h) MATLAB

Figure 2.28: Modes 5 to 8.

Comments

Since the method involves graphical procedures, it can be heavily affected by the amount of damping: the peaks can become very low and wide with high damping values and this makes their detection difficult.

For this reason, the method appears to be suitable for lightly damped structures, like steel or aluminium ones, since the damping contribution carried by these materials is usually quite low.

2.8.3 Steel plate

A $300 \times 250 \text{ mm}^2$ steel plate has been divided 24 ($50 \times 50 \text{ mm}^2$) squares. In this way 35 points have been defined. These locations are used as input/output points, but, when the accelerometers are placed in points that don't belong to the grid, additional input points are defined.

The plate has been tested with different setups:

- 1) 40 impact points and 7 output channels;
- 2) 35 impact points and 2 output channels.

It is important to remark that it is practically impossible to measure the whole FRF matrix. When a hammer test is performed, it is common practice to use many impact points, but using many accelerometers would be very difficult, due to the presence of a lot of wires and the difficulty to hit the plate without touching any accelerometer.

Even in this case, the reference values have been calculated with the RFP-Z method already present in *ARTEMIS Modal*.

Case 1) Figure 2.29 shows the test setup used for this analysis. Table 2.11 shows the results of the computation coming from the PSD fitting method. Modes 1, 2, 10 and 11 have not been detected by the automatic procedure, but they have been picked manually, so they do not appear as picked in the CMIF plot in Figure 2.31 and, as a consequence, in the MAC matrix in Figure 2.30. Besides this, the results related to mode 1 come from the logarithmic decrement method, because mode 1 and 2 are close and a few points represent the first mode: this causes a PSD fitting method failure.

As regards mode 3, it has been automatically found by *ARTEMIS Modal*, but, by looking at the provided MAC matrix, it appears to be highly correlated to mode 2; this is clear also by watching their mode shapes, that look very similar. For this reason, since it has a higher complexity, it has been manually eliminated and doesn't appear in Table 2.11. This same issues happens for modes 4, 5 and 7, that come always in couples in *ARTEMIS Modal*: for each couple, the mode with higher complexity has been manually eliminated; it important to notice that, for each couple, the developed method automatically detects just one mode.

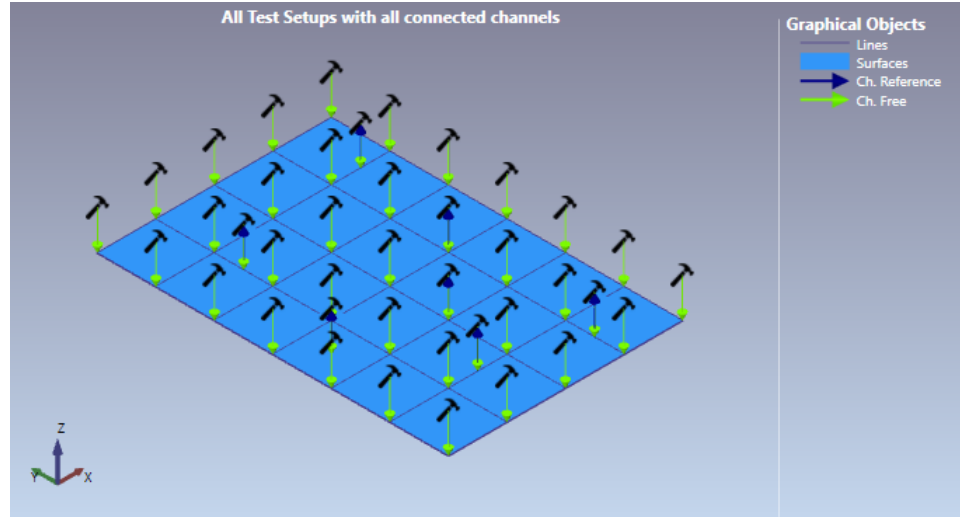


Figure 2.29: Test setup with 40 impact points and 7 output channels.

As regards mode 13, it has been labeled by *ARTEMIS Modal* as a *noise mode*, due to its high complexity; since the developed method does not perform any check on complexity, the mode has been detected.

In general, the results can be considered acceptable for almost every mode.

Mode	Natural frequency [Hz]			Damping ratio [%]		
	Reference	Experimental	Δ [%]	Reference	Experimental	Δ [%]
1	69.85	72.34	3.57	5.878	5.945	1.14
2	88.46	88.50	0.05	6.298	2.157	65.75
3	-	123.90	-	-	7.360	-
4	360.41	360.53	0.03	0.451	0.452	0.15
5	466.76	466.81	0.01	0.334	0.335	0.25
6	699.05	698.69	0.05	0.330	0.332	0.65
7	846.94	846.66	0.03	0.152	0.170	12.08
8	968.98	968.70	0.03	0.127	0.142	11.54
9	1316.39	1316.01	0.03	0.163	0.197	20.98
10	1639.55	1638.90	0.04	0.206	0.210	1.94
11	1649.21	1649.08	0.01	0.214	0.217	1.40
12	1876.79	1876.38	0.02	0.198	0.196	1.24
13	-	2013.17	-	-	0.272	-

Table 2.11: Steel plate results with 40 impact points and 7 output channels.

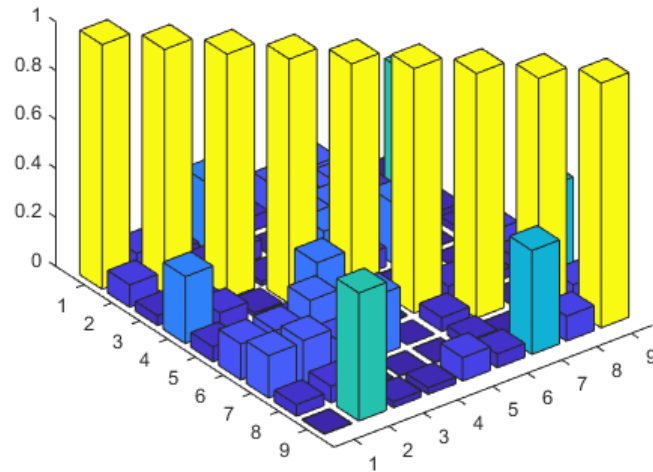


Figure 2.30: MAC matrix of the steel plate with 40 impact points and 7 output channels.

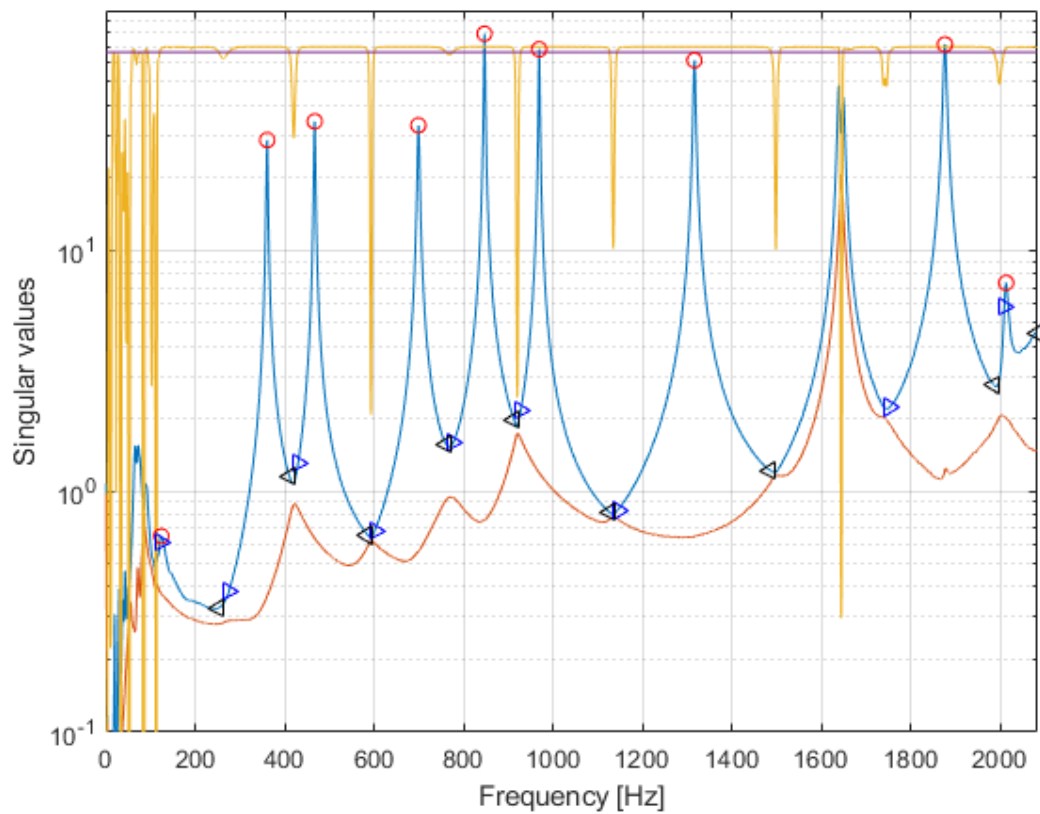


Figure 2.31: CMIF plot with Modal Coherence of the steel plate with 40 impact points and 7 output channels.

Case 2) Figure 2.32 shows the test setup used for this analysis. It is important to notice that the accelerometers are placed in symmetrical positions on the edges of the plate. Table 2.12 shows the results of the computation coming from the PSD fitting method. Modes 4, 5, 7, 9 and 11 have not been detected by the automatic procedure, but they have been picked manually, so they do not appear as picked in the CMIF plot in Figure 2.34 and, as a consequence, in the MAC matrix in Figure 2.33.

In *ARTeMIS Modal*, modes 4 and 6 come in couples: for each couple the mode with higher complexity has been manually eliminated; it is important to notice that, also in this case, for each couple, the developed method automatically detects just one mode.

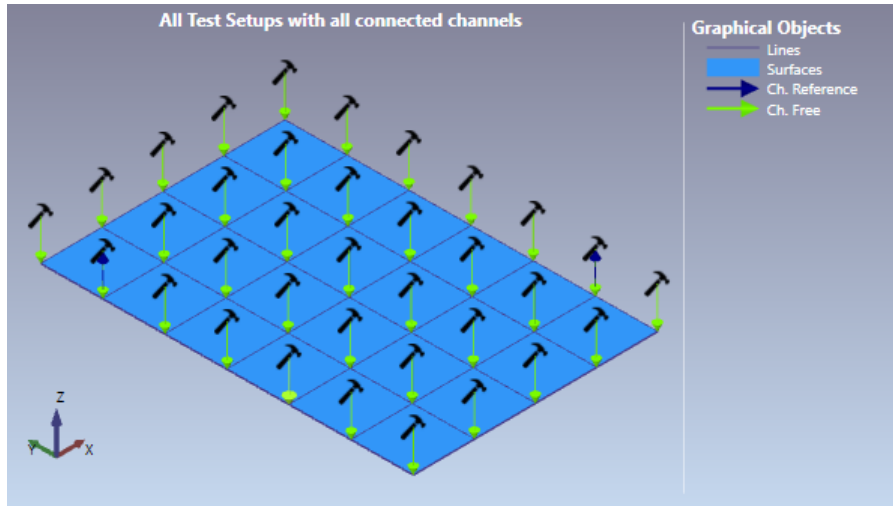


Figure 2.32: Test setup with 35 impact points and 2 output channels.

By observing the MAC matrices in Figure 2.33 it is clear that the results are completely unuseful and not reliable, since there are a lot of high values out of the main diagonal. Since one possible reason could be the symmetrical positions of the accelerometers, a test has been performed with different sensor positions: 7 modes have been automatically detected instead of 5, but even in that case the MAC matrix is way far from being diagonal. For this reason, it is possible to state that the only reason for such bad results is the lack of output channels.

Also the results of the computation, that have been obtained with the PSD fitting method, appear confused: some of them are close to the reference values, some other are very far from them.

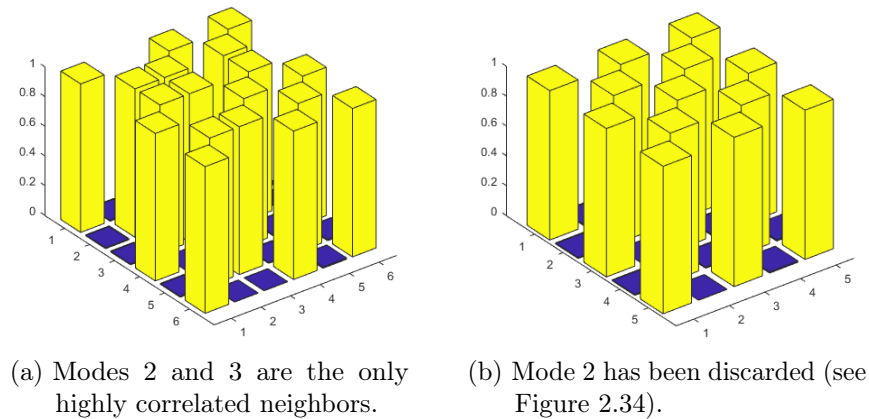


Figure 2.33: MAC matrix before and after the last check.

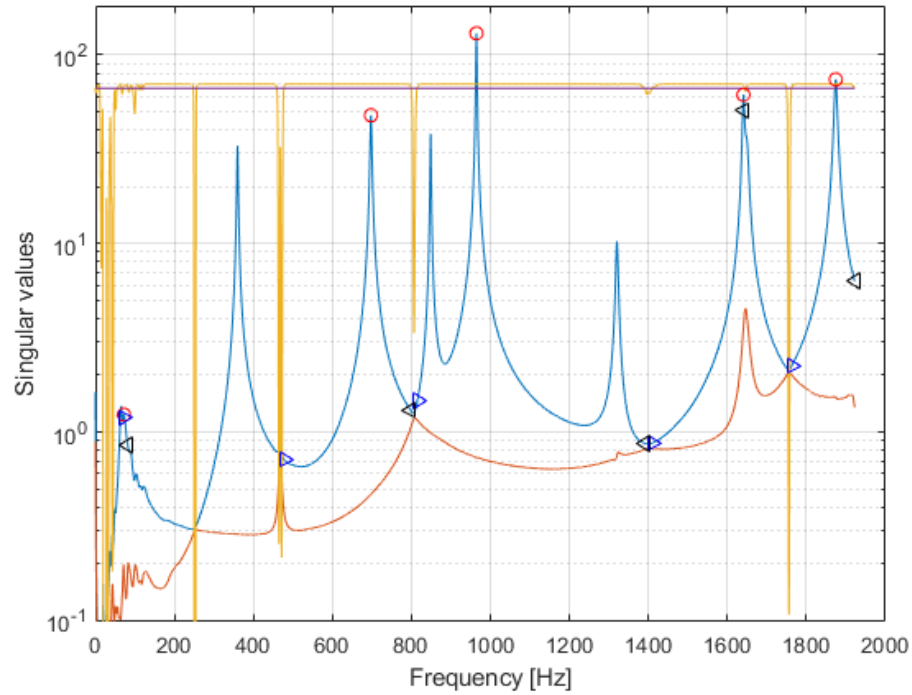


Figure 2.34: CMIF plot with Modal Coherence of the steel plate with 35 impact points and 2 output channels.

Mode	Natural frequency [Hz]			Damping ratio [%]		
	Reference	Experimental	Δ [%]	Reference	Experimental	Δ [%]
1	68.13	72.38	6.25	6.734	5.197	22.83
2	-	-	-	-	-	-
3	-	-	-	-	-	-
4	359.83	360.02	0.06	0.449	0.446	0.58
5	468.19	467.98	0.04	0.299	0.327	9.33
6	697.77	697.51	0.04	0.296	0.311	4.92
7	848.81	848.65	0.02	0.164	0.149	8.90
8	964.68	964.59	0.03	0.207	0.136	34.12
9	1320.76	1320.39	0.03	0.213	0.228	7.23
10	1640.98	1640.51	0.03	0.144	0.175	21.40
11	1650.04	1645.69	0.26	0.254	0.442	74.10
12	1874.40	1874.27	0.01	0.210	0.187	11.03
13	-	-	-	-	-	-

Table 2.12: Steel plate results with 35 impact points and 2 output channels.

Chapter 3

EMA and OMA comparison

3.1 Basic concepts

As already explained, there are two big families of workflows in modal analysis: EMA and OMA. The main difference between them is the nature of the processed data: in EMA the classic FRFs are used, that carry information about both the input excitation and the measured output response, while in OMA only the output response is measured and processed.

This peculiarity makes OMA especially suitable for the analysis of structures in their real working conditions, advantage that is very important for big or heavy structures that can not be brought in a laboratory or in all the situations in which the input is not measurable. In these conditions, the input has to satisfy some requirements, but basically it has to be a white noise [1].

Theoretically speaking, EMA and OMA should give the same results but in practice this is almost never true. In EMA, the input is considered, so if it contains components with high energy at a certain frequency, their effect is reflected on the output. When the FRFs are computed, this effect disappears, since the FRFs are basically the ratio between the output and the input.

In OMA, instead, this effect can not be eliminated, since the input is not measured; for this reason, the input should be a white noise, that has a flat spectrum. Anyway, since this method is used to investigate structures in their real working conditions, some external influences can be present in the output, such as rotating machinery. These energetic components can be easily confused with resonance peaks, so commercial OMA softwares are often equipped with harmonics detection tools. Nevertheless, user's experience is obviously very important.

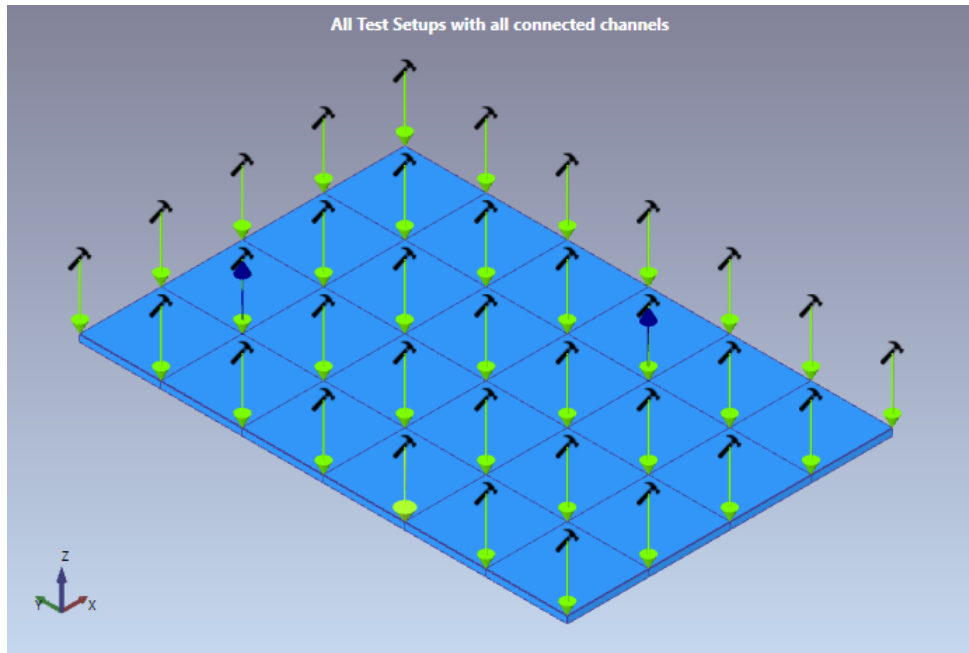


Figure 3.1: *ARTeMIS Modal* screenshot showing the geometry and the channels in the EMA measurement: the green arrows represent the impact points and the blue ones the positions and the directions of the two accelerometers.

3.2 Description of the comparison

In this part of the work, a comparison between EMA and OMA is carried out.

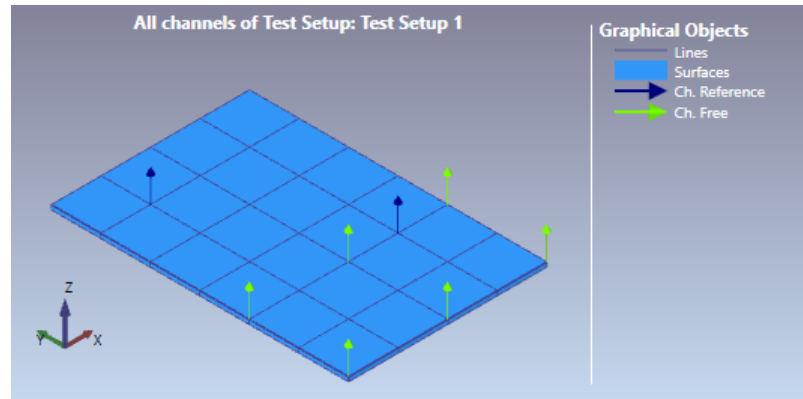
Measurements have been performed on a rectangular steel plate. The EMA ones have been performed, as already said, with 2 accelerometers (outputs) and 35 impact points (inputs), as shown in Figure 3.1. The impacts are generated by hitting the plate by means of an instrumented hammer, in order to measure the input.

The OMA has been performed using two different setups: in both of them two out of eight accelerometers are placed in the same positions in order to use them as reference channels and the other six have been placed in symmetrical positions with respect to one of the symmetry axes of the plate, as shown in Figure 3.2.

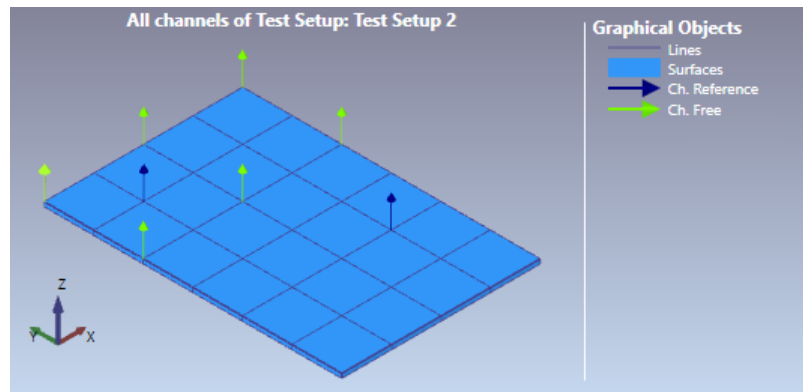
The compared methods are RFP-Z for EMA, and EFDD (**E**nhanced **F**requency **D**omain **D**ecomposition) and SSI-UPCX (**S**tochastic **S**ubspace **I**dentification-**E**Xtended **U**nweighted **P**incipal **C**omponent) for OMA.

3.3 Results

From Tables 3.1 and 3.2 it can be noticed that the natural frequencies are usually very similar between EMA and OMA, except the first one. A possible reason for such a big difference can be the fact that it is much lower than the Nyquist frequency, that



(a) Test Setup 1.



(b) Test Setup 2.

Figure 3.2: *ARTEMIS Modal* screenshots showing the geometry and the channels in the OMA measurements.

corresponds to $f_s/2 = 2500 \text{ Hz}$. As already explained, in fact, it is quite common to have bad data at low frequencies, also due to noise. As regards the damping ratios, the relative differences are always quite big and this is probably caused by the fact that all of them are quite small. By comparing the results coming from EFDD and SSI-UPCX between them, in fact, the relative differences between the natural frequencies are always lower than 1% while those between the damping ratios are of the same magnitude order as those shown in Tables 3.1 and 3.2. In this way is possible to conclude that the big differences between EMA and OMA results for what concerns the damping ratios do not depend on the analysis type.

Mode	Natural frequency [Hz]			Damping ratio [%]		
	RFP-Z	EFDD	Δ [%]	RFP-Z	EFDD	Δ [%]
1	82.22	61.21	25.56	5.529	6.235	12.77
2	359.60	356.73	0.80	0.483	0.501	3.73
3	470.65	465.95	1.00	0.464	0.455	1.94
4	701.25	692.71	1.22	0.366	0.345	5.74
5	850.15	839.61	1.24	0.217	0.233	7.37
6	970.70	957.35	1.38	0.201	0.232	15.42
7	1319.43	1304.93	1.10	0.216	0.297	37.5
8	1644.05	1624.02	1.22	0.166	0.091	45.18
9	1652.50	1631.88	1.25	0.176	0.199	13.07
10	1881.77	1868.83	0.69	0.158	0.636	302.53
11	2158.66	2136.45	1.03	0.179	0.326	82.12

Table 3.1: Comparison between RFP-Z and EFDD.

Mode	Natural frequency [Hz]			Damping ratio [%]		
	RFP-Z	SSI-UPCX	Δ [%]	RFP-Z	SSI-UPCX	Δ [%]
1	82.22	61.74	24.91	5.529	21.662	291.79
2	359.60	356.87	0.76	0.483	0.317	34.37
3	470.65	465.08	0.97	0.464	0.322	30.60
4	701.25	692.79	1.21	0.366	0.244	33.33
5	850.15	839.57	1.25	0.217	0.14	35.48
6	970.70	957.08	1.40	0.201	0.174	13.43
7	1319.43	1304.88	1.10	0.216	0.239	10.65
8	1644.05	1624.41	1.56	0.166	0.46	177.11
9	1652.50	1631.05	1.24	0.176	0.32	81.82
10	1881.77	1868.68	0.64	0.158	0.544	244.30
11	2158.66	2136.65	0.93	0.179	0.499	178.77

Table 3.2: Comparison between RFP-Z and SSI-UPCX.

Acknowledgements

I would like to acknowledge the support provided by my main supervisor Prof. Alessandro Fasana, my foreign supervisor Prof. Lars Damkilde from Aalborg University (DK), my internship tutor Dr. Palle Andersen and Structural Vibration Solutions A/S staff for the pleasant hospitality and for the great opportunity they have given to me.

I would like also to thank my fellow students and friends Pierpaolo and Luca for being always helpful and all my friends from Collegio Einaudi, that, thanks to them, is my home away from home.

Thank you also to Claudio, Simone and Francesca, my Italian-Danish friends, who I've had great time with during my semester in Denmark.

Finally, I am greatly indebted to my family, that has always supported and motivated me during the preparation of the Final Project and in all my academic career, helping me going through all the personal and academic difficulties of these five years. I will always be grateful for the inexhaustible faith they had in me.

Bibliography

- [1] Fasana A., Marchesiello S., *Meccanica delle vibrazioni*, CLUT, 2006.
- [2] Allemang R.J., Brown D.L., *A Complete Review of the Complex Mode Indicator Function (CMIF) with Applications*, University of Cincinnati.
- [3] Allemang R.J., *The Modal Assurance Criterion – Twenty Years of Use and Abuse*, Sound and vibration, August 2013.
- [4] Fasana A., *ZfittingPSD documentation*.
- [5] Andersen P., Brincker R., Goursat M., Mevel L., *Automated Modal Parameter Estimation for Operational Modal Analysis of Large Systems*, Proceedings of the 2nd International Operational Modal Analysis Conference, 2007.
- [6] Fasana A., *Vibration Mechanics course material*.